Groundwater Response to Climate Change and Anthropogenic Forcing: A Case Study on Georgia, U.S.A.

by

Collin Ross Sutton

A thesis submitted to the Graduate Faculty of
Auburn University
in partial fulfillment of the
requirements for the Degree of
Master of Science

Auburn, Alabama
May 5, 2019

Keywords: Groundwater, Climate, Southeastern United States, Georgia, Irrigation

Approved by:

Dr. Ming-Kuo Lee, Chair, Professor of Geosciences
Dr. Sanjiv Kumar, Assistant Professor of Forestry and Wildlife Sciences
Dr. Christopher Burton, Assistant Professor of Geosciences

Abstract

This study analyzed the effects of climate variability and human activities (i.e., irrigation) on groundwater levels from 1981-2017 in four distinct geologic provinces of Georgia. Georgia is located in the southeastern United States and is home to around 10 million people and the country's 9th most populous metropolitan area according to U.S. census data. The southeastern United States has long been thought to be resilient to the types of groundwater issues that are seen in the western United States and around the world. Global climate trends are expected to cause increases in temperature and greater variability in precipitation. While climate change trends are expected to affect groundwater, the exact effects are unknown and are likely to vary significantly based on location and local geology. Declines in streamflow and aquifer storage have already been linked to agricultural irrigation expansion in southwestern Georgia.

Data from a total of 404 USGS groundwater monitoring wells have been collected and analyzed for water table fluctuations over a period of 37 years (1981 to 2017). Gravity Recovery and Climate Experiment (GRACE) data were used to estimate changes in terrestrial water storage in comparison with water level fluctuations. High resolution PRISM (Parameter elevation Regression on Independent Slopes Model) climate data (precipitation and temperature) were also collected for trend analysis at 43 monitoring sites. Long-term and annual groundwater trends are computed using a combination of time series analysis, the Mann—Kendall test, and

autocorrelation analysis. Statistical trends in climate and hydrological data are used to explore the relationship between climate variability, streamflow, and groundwater level.

Time series analyses show statistically significant declines in groundwater level in Coastal Plain and Floridan aquifer systems across the state. The deep confined Coast Plain aquifer appears to be decoupled from climate influences and show the strongest declines in water level. The shallower and less confined Floridan aquifer system appears to be coupled with climate yet also shows declines in water level. By contrast, the Surficial aquifer system and the Northern aquifer system both show relatively neutral trends over the same period. The water table in these shallower aquifers correspond to changes in precipitation. Streamflow data from 36 gauging stations in Georgia show decreasing minimum streamflow trend while other statistics show no trends. Statewide precipitation was found to show no significant trend and temperature averages were shown to show slight increases in nighttime averages, indicating non-climate factors has likely caused the groundwater declines in deeper, confined aquifers. Autocorrelation analysis indicates that each aquifer system and precipitation tend to have different durations of memory. The precipitation and unconfined aquifers exhibit the shortest duration of memory ranging from 3 to 6 months, while the deeper confined aquifers show substantially longer memory and significant lag times of 12 to 18 months or greater. Statistically significant decreasing trends in water level and long lag times further indicate groundwater in deeper aquifers is decoupled from climate influences.

Acknowledgments

This research was supported by a grant from the National Science Foundation (NSF-1425004) which was integral to the execution of this research and supported my graduate assistantship. This research would not have been possible without the help of my thesis committee: Dr. Ming-Kuo Lee, Dr. Sanjiv Kumar, and Dr. Christopher Burton. First, a special thanks to the chair of my committee, Dr. Lee, who was a source of constant guidance and support. Dr. Lee's first priority was mentorship and it is apparent in all that he does. My success at Auburn is directly attributed to Dr. Lee's passion for helping students. Secondly, thanks is also owed to Dr. Kumar. Dr. Kumar was pivotal to my understanding of the programming languages and statistics. Lastly, I would like to thank Dr. Burton for his support and mentorship throughout this process.

I would also like to thank Dr. Ashraf Uddin for allowing me the opportunity to participate on the Imperial Barrel Award team which has left me with fond memories and essential skills that I will carry with me as I begin my career. A special thanks is owed to all of my friends, both new and old, who have helped me along during this journey. Without this constant source of joy and support, this process would have been much more difficult and much less enjoyable. I must also thank my family who helped push me academically and morally from a young age. Without these people and countless others this research and my graduate experience would not have been possible and as fulfilling.

Table of Contents

List of Tables

List of Figures

Chapter 1: Introduction

Groundwater is an important natural resource and is an integral part of the global freshwater supply (Gurdak et al., 2009). Understanding how human impacts and climate change and variability affect groundwater and water resources in general is important due to the complexity of the systems involved and the significance of freshwater (Dragoni and Sukhija, 2008). The availability of groundwater depends heavily on the climate, local geology, and human interaction (Leeth et al., 2007; Melillo et al., 2014). Around 20 percent of projected freshwater scarcity can be linked to climate change (Sophocleous, 2004). Sandstrom (1995) showed that as little as a 15 percent reduction in precipitation could lead to around 40 to 50 percent less groundwater recharge in semiarid to arid climates. Additionally, growing population has caused overpumping which leads to decrease in groundwater and saltwater intrusion in coastal areas (Denizman, 2018).

Scientific consensus on climate change is that the global temperature will increase leading to an increase in regional precipitation variability, both positively and negatively (Green et al., 2011; IPCC, 2014). For example, seasonal variations of increased precipitation will lead to more recharge and less need for groundwater use (Rosenburg et al., 2008). Alternatively, variations in precipitation will lead to more extreme drought especially in areas such as the continental interior (IPCC, 2007a; Bates et al., 2008). Recurring changes in climate cycles (e.g., El Niño/Southern Oscillation (ENSO), Pacific Decadal Oscillation (PDO), and Atlantic Multidecadal Oscillation (AMO), Northern Atlantic Oscillation (NAO), etc.) can result in short-term and long-term climatic influences and can dramatically affect precipitation and groundwater (Wolter and Timlin, 1993; Wolter and Timlin, 1998; Hanson et al., 2003; Gurdak et al., 2007). For example, ENSO cycles are the primary factor in the Southeastern United States leading to drought conditions and has been shown to correspond with water table fluctuations (Mitra et al., 2014).

In the United States, groundwater is responsible for up to 40 percent of the freshwater supply with as many as 40 million people drinking groundwater (Alley et al., 1999; Gurdak et al., 2009). Irrigation alone accounts for 60% of this freshwater use (Braneon, 2014). According to work done by Brekke et al. (2009), many principal aquifers around the country are in danger of depletion due to natural climate variability and anthropogenic climate change. In the western U.S., short to long-term drought has been shown to cause irrecoverable, significant declines of water table in the Central Valley aquifer in California in as little as a 30 year observation period (Miller et al., 2009). The high plains aquifer (Ogallala aquifer) that covers more than 450,000 km^2 in eight states of the central United States has shown continual decline in water table depths since the 1950's to present; in some areas the decline is 50 m or greater (Sophocleous, 2010).

The 'water rich' southeastern U.S. has long been thought to be immune to these kinds of climatic effects on surface-water and groundwater (Ingram et al., 2013; NWF, 2008). The Southeast's population is expected to grow by 24% in the next 20 years and land use patterns are changing; for example, urban area has increased by 200% from 1945 to 1992 (Wear, 2002; Sun et al., 2008). Human land use and change, including irrigation, has been shown to affect local, regional, and potentially global climate through surface and air temperature changes, modifying partitioning of net radiation into evapotranspiration rates and heat fluxes, and the precipitation efficiency (Kumar et al, 2010; Mahmood et al., 2016; Cook et al., 2015). High levels of irrigation have been shown to cause aquifer storage loss, changes in groundwater flow (i.e. gaining stream to losing stream), decreases in stream baseflow, and decreases in aquifer recharge (Mitra et al., 2016; Mitra et al; 2019)

Climate variability and change is causing shifting perspectives on the Southeast's supply of water (Mitra et al., 2014; Singh et al., 2015). The Southeast is expected to see an increase in

hurricane intensity, precipitation variability, change in vegetation, and salt-water intrusion from rising ocean levels in addition to the effects of raising temperature (i.e., higher evapotranspiration, declining runoff, and increased water demand) (Ingram et al., 2013). While the effects of climate variation on the Southeast has been studied in some detail, there is little in the literature discussing its effects on the groundwater in this region.

The work conducted for this research seeks to fill the gap in the existing knowledge with the assessment of a large dataset of long-term groundwater monitoring wells across the state of Georgia by integrating big data techniques with historical hydrogeologic, climate observations, and land use change. A total of 404 USGS groundwater monitoring wells have been collected, out of which 43 wells had long-term data availability for the recent historical period (1981 to 2017) and were analyzed for the changes in water table. A dataset of this size allows for the opportunity to assess the role of natural and anthropogenic forcings (e.g. land use change and irrigation) by testing the hypothesis that groundwater fluctuations should be a function of climatic cycles and any deviation from this may be attributed to anthropogenic forcing.

Statistical trend analysis, autocorrelation, and time series analysis were used to test this hypothesis. Since, the ground water time series is expected to show a high degree of persistence (autocorrelation), a statistical technique was used that considers long-term persistence in the time series (Kumar et al., 2009; Kumar et al., 2013) to investigate secular changes in the ground water availability in the region. Seasonal autocorrelation analysis (Kumar et al., 2019) is employed to characterize memory time scale or the persistence in the different aquifer system in Georgia. A review of the literature indicates this is first study that investigate long-term changes in the ground water in the humid part of the United States and using big data techniques. Since it is important to understand the study area, the geology, hydrogeology, climate, and anthropogenic forcings is first

introduced in chapter 2. Then, after summarizing the research methodology and available datasets in chapter 3, the results of the analysis will be presented and discussed in chapter 4. Finally, chapter 5 presents a summary and brief conclusion of my findings, noting key limitations of this study and suggestions for future investigation.

Chapter 2: Background

Geology and Hydrogeology

Georgia consists of four distinct geologic regions (Figure 1 and 2A) beginning with the Coastal Plain spanning from the Fall Line to the Atlantic Ocean and into Florida, the Piedmont throughout the central area of the state, the Blue Ridge in the northeast, and finally the Valley and Ridge in the northwest. The Coastal Plain consists of mostly layered sand, clay, and limestone which thickens up to 1.5 km in depth to the southeast; those sediments are derived from the weathering of the Appalachian Mountains and repeated transgressive and regressive cycles (Clarke and Pierce, 1985).

Within the Coastal Plain lies the surficial aquifer system, Brunswick, Floridan, Gordon, Claiborne, Clayton, Cretaceous aquifer systems, among several others (Figure 1) and they are the most productive aquifers in the state (Gordon and Painter, 2018). These aquifers can essentially be categorized as 3 distinct aquifer systems: the Floridan aquifer system (carbonate rocks), the Coastal Plain aquifer system (clastic rocks), and the surficial aquifer system (Williams and Dixon, 2015). Aquifers in the Coastal Plain are typically confined except for in the northern extent of the Coastal Plain and the surficial aquifer system (Clarke and Pierce, 1985). The surficial aquifer system is comprised of post-Miocene aged deposits and are categorized 3 ways: 1) Pliocene marginal marine to shallow marine; 2) Pleistocene marine terrace deposits; and 3) Holocene fluvial and residuum deposits (Williams and Dixon, 2015). The remainder of the state north of the Fall Line also has a surficial aquifer system which is composed of soil, saprolite, alluvium, colluvium, and surficial deposits (Gordon and Painter, 2018).

The Floridan aquifer system, one of the most productive in the U.S., underlies the southern half of Georgia, is mainly used as the primary source of fresh water, and is characteristically

carbonate (Miller, 1986; Fanning, 2003). The Floridan aquifer system is separated into the Upper and Lower Floridan aquifers. The Upper Floridan aquifer is of Eocene to Oligocene aged limestone, dolomite and calcareous sand (USGS Fact Sheet, 2006). The Lower Floridan Aquifer is defined as the unit under the Middle Floridan Confining Unit which is exposed at the surface in some portions of southeast Georgia as part of the Floridan aquifer system (Miller, 1988).

The Upper Floridan aquifer is confined in areas where it is overlain by siliciclastic sediments or a low-permeability Miocene aged limestone and is unconfined at surface outcrops at the northern extent of the aquifer and through karst features to the southwest and southcentral parts of Georgia (Miller, 1986; Williams and Dixon, 2015; Denizman, 2018). The aquifer thickens to the southeast up to a maximum depth of around 500 meters (Miller, 1986). Interestingly, although the Floridan is a karst aquifer, it has been shown to have significant primary and secondary porosities (Denizman, 2018).

The Southeastern Coastal Plain aquifer system is composed of a thick wedge of unconsolidated to poorly consolidated Jurassic to Holocene clastic rocks that dips to the southeast from the Fall Line to the Atlantic Ocean (Renken, 1996). The Coastal Plain aquifer system is overlain by the Floridan aquifer system and both are hydraulically interconnected laterally (Floridan carbonates to the south which grades into Coastal Plain clastics of the same age to the north) and vertically (gradual gradations or interfingering between clastics and carbonates) and underlain by crystalline bedrock (Renken, 1996). The Lower Floridan aquifer and the Coastal Plain aquifer system are connected laterally while the Upper Floridan aquifer and the Coastal Plain aquifer system are connected vertically (Renken, 1996). Due to this connection, the Coastal Plain aquifer system rocks are both clastic and carbonate especially in the south and southwestern portions of Georgia (Renken, 1996). Much of the northern half of the state is represented by the

Piedmont and Blue Ridge Provinces. The Piedmont and the Blue Ridge are classified by low to high grade metamorphism with the exception of localized plutons such as Stone Mountain (Hatcher, 1978). The aquifers here are typically unconfined and mostly composed of regolith or crystalline-rock aquifers which store water in fractures, joints, contacts, weathered zones, and other features (Clarke and Pierce, 1985; Gordon and Painter, 2018).

The northwestern most extent of the state is represented by the Valley and Ridge Province. The Valley and Ridge is characterized by thrusted and folded parallel ridges underlain by resistant sandstone, conglomerate, or cherty dolostone and valleys underlain by siltstone, shale, limestone, or other weathering prone rocks (Rutledge and Mesko, 1996). The aquifer systems are typically unconfined in joints, fractures, and solution openings (Clarke and Pierce, 1985).

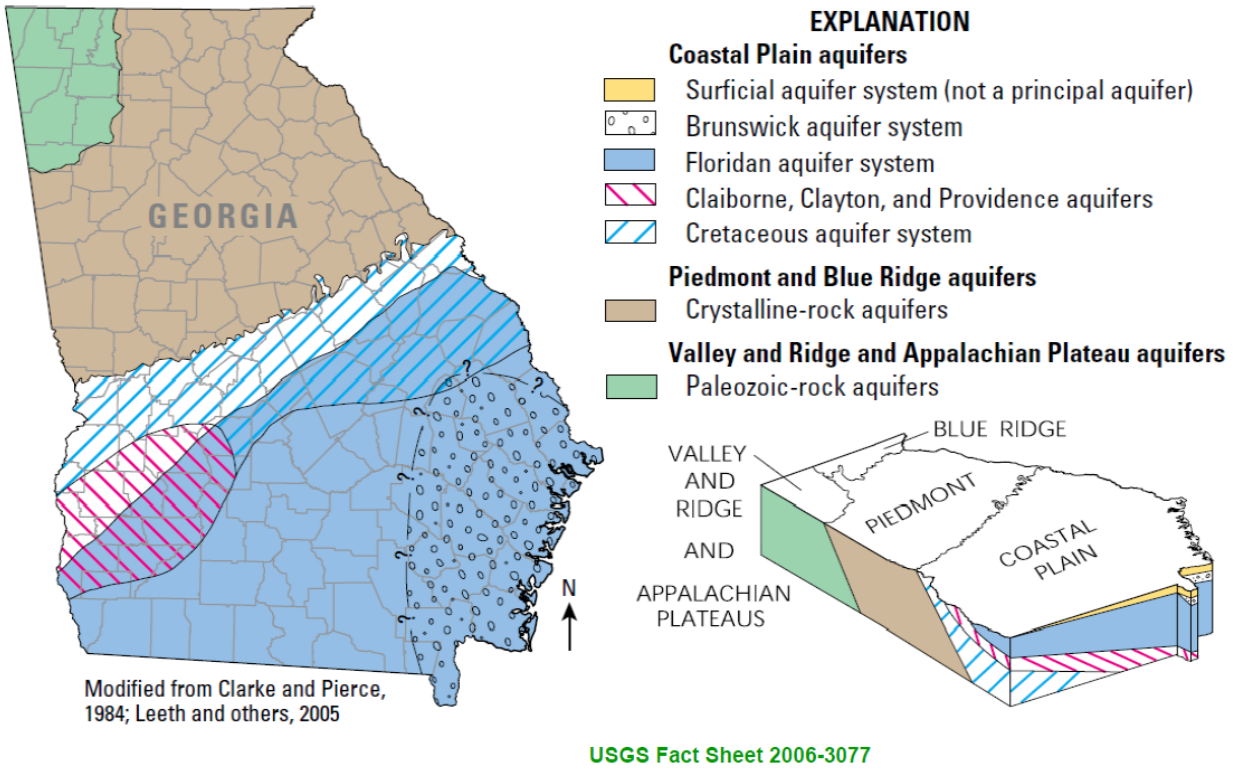

Figure 1. Left side shows a map of Georgia, U.S.A., showing the distinct hydrogeologic provinces of Georgia. The Claiborne, Clayton, Providence, and Cretaceous aquifer systems are defined as the Coast Plain aquifer system in this study. Bottom Right Corner shows aross-section view of Georgia showing the 4 distinct Geological Provinces on the top and the stratigraphic relationships of the aquifer units on the sides.

Climate and Anthropogenic Forcings

Previous literature has focused heavily on the interactions between climate and surface water due in large part to the availability of data and the water itself, however recent studies have begun to investigate the interactions between climate and groundwater (Green et al., 2007; Gurdak et al., 2009). Studies in the U.S. have found that global climate change will lead to water storage and supply issues in arid and semiarid environments – while other areas are understudied. Climate change and variability will be a factor in long-term groundwater sustainability over broad areas, and will also change groundwater flow patterns in coastal areas due to saltwater intrusion, future pumping, and sea level rise (Loaiciga et al., 1996; Alley, 1999; Sherif and Singh, 1999; Burnett et al., 2006).

The Southeastern United States typically has high amounts of annual precipitation (43 in. to 54 in. on average), limited seasonality, interannual variability, and the region can have seasonal to annual length droughts (Labosier and Quiring, 2013; Ford and Labosier, 2014,). Winter and summer precipitation and temperature variability tend to be influenced by different mechanisms: El Nino-Southern Oscillation (ENSO) drives winter variability and there is a lack of clear consensus on the drivers of summer variability (Ford and Labosier, 2014). Positive phases of ENSO (El Nino) correspond to cooler, wetter winter conditions in the southeast and negative phases of ENSO (La Nina) correspond to warmer, drier winter conditions in the Southeast. ENSO has been shown to have a strong relationship with shallow to moderately deep aquifers in southwest Georgia; El Nino phases have been shown to correspond to higher than average water table while La Nina phases have been shown to correspond to lower than average water table level (Mitra et al., 2014).

Summer precipitation variability has increased in recent decades due to a combination of Atlantic Ocean sea surface temperature variability, the North Atlantic subtropical high pressure cell, and the Atlantic Multidecadal Oscillation (McCabe et al., 2004; Wang et al., 2010; Diem, 2006; Diem, 2013; Ford and Labosier, 2014). Studies have also identified that ENSO coupled with other cycles such as AMO and NAO can significantly lower baseflows during La Nina phases paired with positive PDO and AMO phases and increase baseflows during El Nino phases coupled with negative PDO and AMO (Singh et al., 2015).

Historically the average temperature of Georgia and the southeast showed no warming or even cooling trend over the majority of the 20th century (Kunkel et al., 2013). However, taking into account only 1975 to present (Figure 2D), there is a warming trend of around 2 degrees F that is projected to continue to rise 4 to 8 degrees F (Kunkel et al., 2013) in the next 100 years. The expectation is an increase in hot days (>95 degrees F) and a decrease in freezing events (Melillo et al., 2014). Annual precipitation (Figure 2C) in the Southeast shows a slightly positive trend from 1895-2011 according to the Southeast Regional Climate Center. The projected annual change in precipitation for Georgia is slightly positive with a small portion of the state showing statistically significant variation (Kunkel et al., 2013). Very heavy rainfall events (heaviest 1%) have increased across the region by 27% from 1958 to 2012 and models predict that variability in extreme rainfall events is likely to increase in the future (Karl et al., 2009; Kunkel et al., 2013; Melillo et al., 2014).

The projected change of precipitation is expected to be a climatic cause of decrease in groundwater (Van Dijck et al., 2006; Kudezwicz et al., 2007; Ouysse et al., 2010). Groundwater is the major contributor to baseflow of streams and rivers in times of dry conditions and climatic variability and change is expected to impact surface water bodies due to this connection (Lee and Chung, 2007; Dragoni and Sukhija, 2008). Precipitation variability has been shown to cause both

increases and decreases in surface water runoff which will have uncertain effects on regional hydrologic cycles (Chiew and McMahon ,2002; Milley et al., 2005).

Agricultural withdrawals have been shown, typically in semi-arid to arid climates, to be a cause of aquifer depletion in areas where withdrawals exceed the rate of recharge (Siebert et al., 2010). However, agricultural withdrawal has been the major factor in groundwater depletion in other climates such as the North China Plain which has a subtropical monsoon climate (Sun et al., 2010). Agricultural production increased 50% globally from 1960 to 2000 and this increase can be partially linked with a large expansion in irrigation which is also expected to increase by around 50% globally by 2050 (Tillman, 1999; Tillman, 2001).

Increased evapotranspiration from higher surface temperatures is also expected to lead to a larger increase in irrigation water demand by crops and a subsequent extra stress on groundwater (Doll, 2002). A specific example is seen in the Apalachicola-Chattahoochee-Flint (ACF) River Basin which covers much of southwestern Georgia, some of eastern Alabama, and parts of the panhandle of Florida and is encountering declining levels of precipitation, soil moisture, and runoff (Georgkakos et al., 2010). Water demands have risen due to urban growth and irrigation expansion, but climate projections show that a combination of yearlong soil moisture decreases and runoff declines will lead to reduced supplies and increased demands (Georgkakos et al., 2010). Irrigation in the region has already led to around a 20% decrease in streamflow and a caused a change from perennial streams to intermittent streams, losses in aquifer storage, and changes in groundwater flow patterns (Singh et al., 2016; Mitra et al., 2016; Singh et al., 2017; Mitra et al., 2019). In Georgia, acres irrigated have increased from 42,408 acres to 936,245 acres (roughly 2000%) from 1976 to 2013 (Williams et al., 2017). Southwest Georgia, including the ACF basin, is the most

densely irrigated area of the state and most other irrigation was limited to the central and eastern portions of the Coastal Plain (Figure 2B) (Williams et al., 2017).

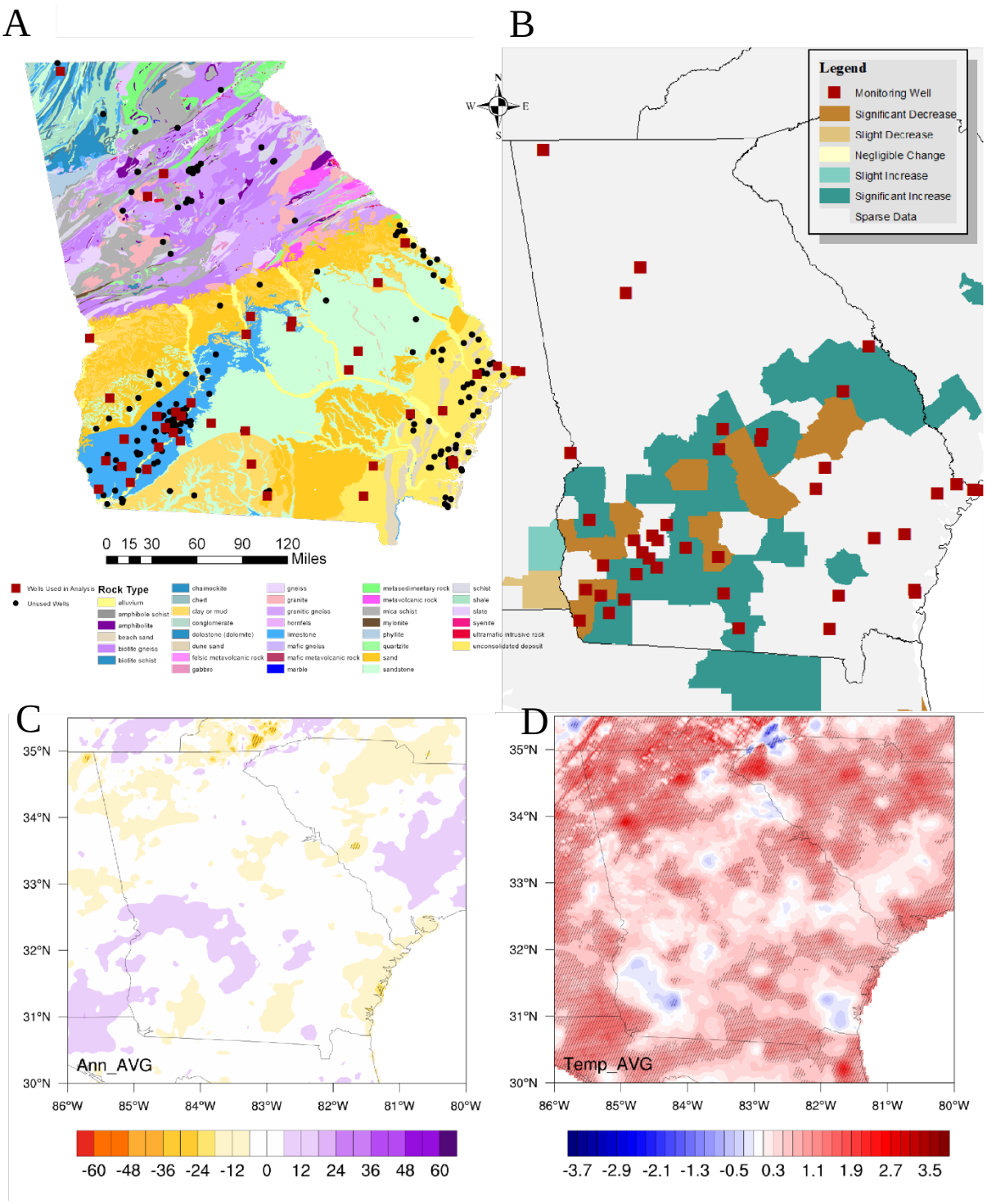

Figure 2. Composite showing (A) the geology of Georgia with locations of groundwater monitoring wells (Black circle: Monitoring well not included in analysis, Red square: Monitoring well included in analysis), (B) Irrigation trend map for Georgia from 2007-2012 (data from USDA Irrigation Survey), (C) Annual average precipitation trend map for Georgia from 1981-2017 (Scale is multiplied by 10 to show exaggerated trend. i.e. 60 represents 6% change, (D) Annual average temperature (day time – night time temperature) map for Georgia from 1981-2017 (Scale represents degree temperature change). (Data from C and D are using PRISM data and statistical significance are based on linear regression trends)

Chapter 3: Research Methodology

Sources of Climate, Geological, and Hydrologic Data

Georgia groundwater table data for 404 monitoring wells were collected from the USGS National Water Information System (NWIS) database (Table 1) (https://www.usgs.gov/water-data-nation-national-water-information-system). The NWIS contains the most complete ground-water-level dataset for the U.S., including data from federal programs and agencies as well as state and local governments. These monitoring wells are spatially distributed in three major hydrogeologic provinces including: the Coastal Plain, Piedmont and Blue Ridge, and Valley and Ridge (Figure 3).

Daily water table measurements were obtained from the database for each well, for the period from 1951 to present; however, most of the wells did not have constant daily measurements over this entire time interval. To include the most wells possible, 43 wells were determined to have 90% or more data available over a time range from 1981 to 2017 (Table 1). All the wells used in this study are designated as monitoring wells which means they are not in use or influenced by human activity and instrumentally record daily water table measurements. The data obtained is given in groundwater depth from the well head, so the data was subtracted from the altitude of the well for the groundwater surface elevation to be determined relative to NAD83. Other information retrieved from the NWIS database includes latitude and longitude for the station, name of regional and local aquifer, and depth of the well.

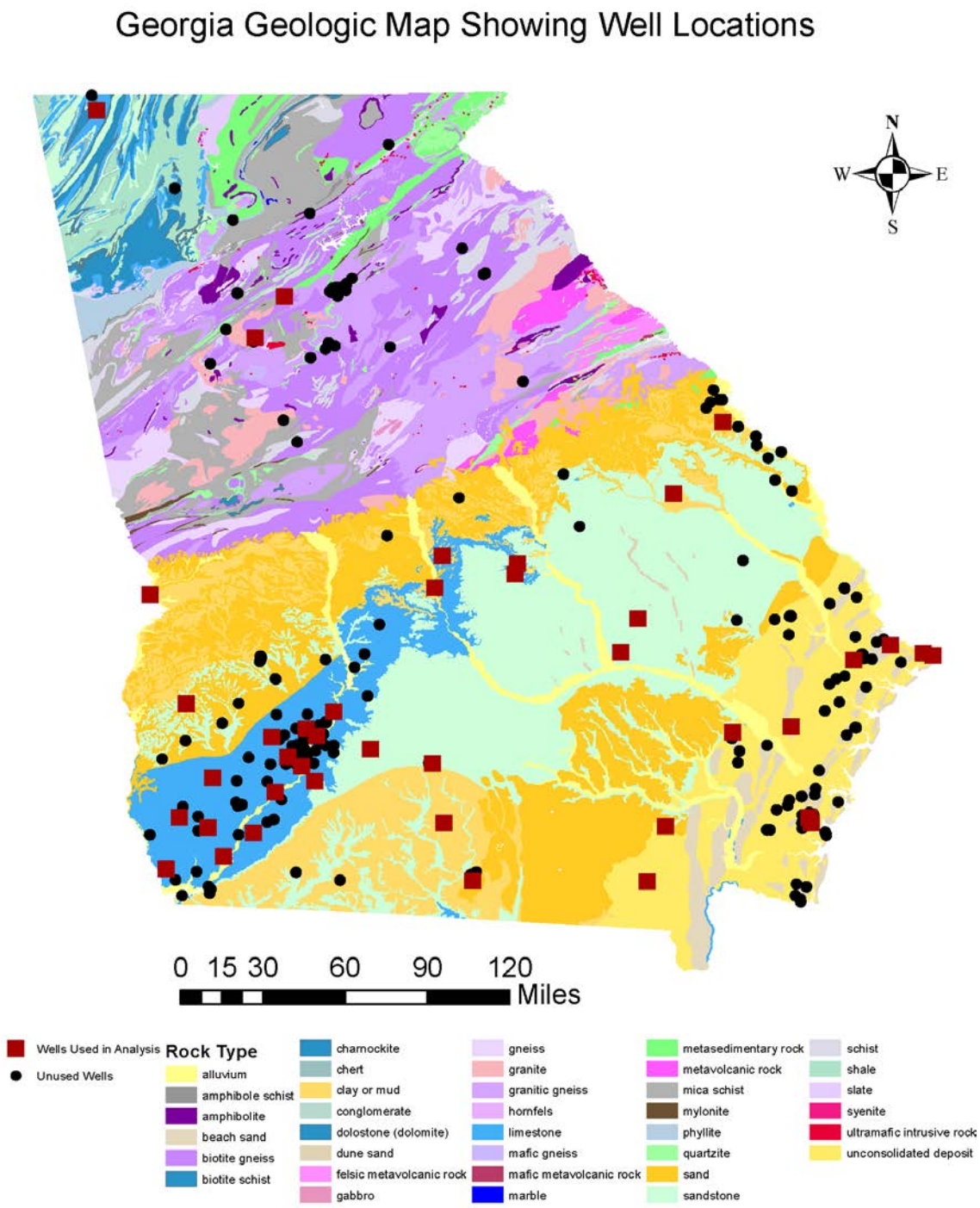

Figure 3: Geologic map of Georgia showing surface geologic units (USGS) and locations of 404 groundwater monitoring wells (unused wells are black and used wells are red).

Table 1 List of USGS groundwater monitoring wells used in study. (Aq.: Aquifer, FAS: Floridan Aquifer System, CPAS: Coastal Plain Aquifer System, SA: Surficial Aquifer, NAS: Northern Aquifer Systems).

SI. No.	Well ID	Site Number	Altitude	Aq.	Local Aquifer
USGS Monitoring Wells					
Georgia Coastal Plain					
1	304942082213801	27E004	116	FAS	Upper Floridan Aquifer
2	304949083165301	19E009	213	FAS	Upper Floridan Aquifer
3	305356084534601	06F001	110	FAS	Upper Floridan Aquifer
4	305736084355801	09F520	128	FAS	Upper Floridan Aquifer
5	310507084262201	10G313	145	FAS	Upper Floridan Aquifer
6	310651084404501	08G001	152	FAS	Upper Floridan Aquifer
7	310706082155101	27G003	150	FAS	Upper Floridan Aquifer
8	310813083260301	18H016	241.42	FAS	Upper Floridan Aquifer
9	310818081294201	34H391	7.13	FAS	Lower Floridan Aquifer
10	311007081301702	33H133	6.71	FAS	Upper Floridan Aquifer
11	311009084495503	07H003	167	SA	Surficial Aquifer
12	311802084192301	11J011	165	CPAS	Claiborne Group
13	311802084192302	11J012	165	FAS	Upper Floridan Aquifer
14	312127084065801	13J004	194	FAS	Upper Floridan Aquifer
15	312232084391701	08K001	230	FAS	Upper Floridan Aquifer
16	312617084110701	12K014	180.3	FAS	Upper Floridan Aquifer
17	312712082593301	18K049	330	FAS	Upper Floridan Aquifer
18	312919084153801	11K003	194.86	FAS	Upper Floridan Aquifer
19	313146083491601	15L020	420	FAS	Upper Floridan Aquifer
20	313532084203501	11L002	222	CPAS	Clayton Group
21	313554084062501	13L002	212.84	CPAS	Clayton Group
22	313701081543501	30L003	105.77	FAS	Upper Floridan Aquifer
23	313808084093601	12M017	225	FAS	Upper Floridan Aquifer
24	313845081361701	33M004	60.3	FAS	Upper Floridan Aquifer
25	314330084005402	13M006	238	FAS	Upper Floridan Aquifer
26	314330084005403	13M007	238	SA	Surficial Aquifer
27	314602084473701	07N001	445	CPAS	Clayton Group
28	315950081161201	35P094	18.67	SA	Surficial Aquifer
29	320122080510204	39Q003	7	FAS	Upper Floridan Aquifer
30	320202080541201	38Q002	8	FAS	Upper Floridan Aquifer
31	320226082301101	25Q001	190	FAS	Upper Floridan Aquifer
32	320433081042701	37Q016	4.7	FAS	Upper Floridan Aquifer
33	321302082243601	26R001	287	FAS	Upper Floridan Aquifer
34	322036084590301	06S001	255	CPAS	Blufftown Formation
35	322245083290101	18T001	334	CPAS	Midville Aquifer
36	322652083033001	21T001	259	FAS	Upper Floridan Aquifer
37	323030083030003	21U004	282	CPAS	Midville Aquifer
38	323302083263401	18U001	444	CPAS	Dublin Aquifer
39	325232082131501	28X001	269	CPAS	Midville Aquifer

40	331711081573701	30AA04	297	CPAS	Grdn, MP, & Dublin Northern Aquifers
41	334207084254801	10DD02	1013	NAS	Crystalline Rocks
42	335517084164001	11FF04	963.05	NAS	Crystalline Rocks
43	345403085160001	03PP01	730	NAS	Chickamauga Limestone

High resolution PRISM climate data were used in this study. PRISM uses a sophisticated regression model called Parameter elevation Regression on Independent Slopes Model to account for complex climate regimes associated with orography, rain shadows, temperature inversions, slope aspect, coastal proximity, and other factors, and interpolates station observation to spatially continuous 4-km grid data (Daly et al., 1997; Daly et al, 1998). For this study, monthly precipitation, temperature maximum, and temperature minimum data were collected for Georgia. Precipitation and temperature trends were determined on a statewide scale using the entire PRISM dataset for the southeastern U.S. Precipitation data was also collected for the nearest PRISM node to each 43 individual groundwater monitoring station for correlation and trend analysis.

Gravity Recovery and Climate Experiment (GRACE) data have been collected to calculate terrestrial water storage time series for comparison with Georgia's groundwater monitoring well data. GRACE land are available at http://grace.jpl.nasa.gov, supported by the NASA MEaSUREs Program (Senson, 2012; Landerer and Swenson, 2012; Swenson and Wahr, 2006). Irrigation data has also been retrieved from the USDA Irrigation Survey (https://www.nass.usda.gov/Surveys/Guide_to_NASS_Surveys/Farm_and_Ranch_Irrigation/) to investigate possible driver or causes of long-term changes in groundwater.

Data Processing

The NWIS generates one ASCII (.txt) file for all data downloaded regardless of size or location; therefore, the raw data must be sorted and processed before they can be used. The data are given with an informational header and water table depth information for every recorded day

and unique well identification number (well ID). The data are listed sequentially by well ID and each well contains its own header. The header for each well is unique and is used here as the point at which the data can be delineated. The Python programming language is used to "clean" the data (appendix 1). Cleaning here refers to separating each well based on the beginning of the header (which is always "# # Data provided for") and the well ID into individual .txt files.

Separating each well ID into individual .txt files is important so that Visual Basic for Applications (VBA) can be used to import the .txt files into Microsoft Excel 2016 as individual worksheets (appendix 2). Individual worksheets were used for each well since Excel has a maximum capacity of 1,048,576 rows of data in one workbook and all the Georgia well data has the potential of having 9,739,229 total rows of data (daily data from 1951 to 2017); however, each well only has the potential of having 24,107 rows of data. VBA is the integrated programming language for Excel and was used throughout the cleaning and processing phase.

VBA was used in a variety of ways to further clean and process the data once the wells data were separated in Excel worksheets. A "Master" sheet was created which has all the information for each well including well ID, site name, type, latitude, longitude, datum, altitude of well head, national aquifer code, local aquifer code, and aquifer type. The "Master" sheet was used as a reference by VBA to ensure that each line of a specific well's workbook corresponds to the well ID from the "Master" sheet. A "Master 2" sheet was created next to allow for the printing of output from VBA and includes: data start date, data end date, number of rows, and number of rows with data. VBA code was developed to determine the amount of daily available data from 1951-2018 for each well and is printed as data start date and data end date and then the percentage of the data that was usable by counting the number of rows with data (appendix 3).

Further VBA code was developed once the data was counted and organized to add in a "null" value that would be specific for the entire dataset (appendix 4). The number "-999.0" was chosen due to the unlikelihood of a -999 ft. depth to water table measurement or water table elevation. The typical appearance of missing data in the code came as a simple blank cell; however, multiple other characters could be given by the NWIS including: "Eqp", "***", and "—". Lastly, the final portion of VBA code was written to write all missing data from 1951 to 2017 so that the entire dataset has the same length and would only include the working data and the null value (appendix 5). All values added from this code can be identified by "CRS" in the final column of each well data worksheet.

Data Analysis and Statistical Methods

Analysis Tool

Data analysis was accomplished using the National Center for Atmospheric Research Command Language (NCL) and MATLAB. NCL is an open source free software for scientific computing. NCL is an interpreted language designed for scientific data processing and visualization (NCAR, 2017) and is one of the available software on Auburn Supercomputer "Hopper". The Georgia groundwater data were exported from excel into individual comma delineated .csv files using open-source VBA code and then groundwater data and metadata (from "Master") were read into NCL using the asciiread function to create a netCDF file (.nc) (appendix 6) with an intent to conduct multi-dimensional analysis. NCL software allows us to conduct analysis across multiple sites, and several ground water statistics together using multi-dimensional data processing techniques.

Metrics

Six sets of groundwater statistics were computed in NCL to determine low, medium, and high-water conditions in Georgia. The low water table condition statistics include 1-day minimum (L1) and 7-day minimum (L7); medium condition statistics include median annual water table (M_{50}) and annual average (M1); and high water table condition statistics include 1-day maximum (H1) and 7-day maximum (H7). This method is adapted from Kumar et al. (2009) for groundwater applications. Additionally, a measure of reliability in ground water availability that is computed as the range between 1-day maximum and 1-day minimum flow is included. A higher range or an increasing trend in the range represent less reliable ground water availability (Kumar et al., 2014). Groundwater table statistics are computed for seasonal and annual durations (appendix 7). Seasonal durations include winter (December, January, February), spring (March, April, May), summer (June, July, August), and fall (September, October, November). All statistics are calculated using groundwater table elevation and are standardized according to:

$$Z = \frac{X - \mu}{\sigma} \qquad (1)$$

where X is the value being standardized (e.g. a groundwater elevation for a given day), μ is the mean of the distribution, and σ is the standard deviation of the distribution.

Additional analysis is preformed using similar metric but for the surface flow (stream flow), temperature, and precipitation data to better understand ground water changes in the context of hydroclimatic changes in the region.

Statistical Methods

The goal of this study is to understand long-term changes or trends in ground water availability and their drivers. Non-parametric trend detection methods have been used to overcome the known deficiency in hydroclimatic time series that do not follow the normal distribution

(Gaussian distribution) particularly for extremes, e.g. 1-day maximum ground water tables. Hydro-climatic time series also show long-term persistence that is clustering of wet or dry events for several years in a row (Kumar et al., 2013; Hurst, 1951). This behavior is particularly important for ground water time series that reflect integration effects due to land memory process and large storage capacity of ground water reservoirs in addition to random climate forcing, and thereby ground water spectrum is red compared to the spectrum of climate forcing which is mostly white (Ghannam et al., 2016; Kumar et al., 2019). Presence of long-term persistence reduces the independent sample size in the time series and there by overestimates significance of trends (Koutsoyiannis and Montanari, 2007; Kumar et al., 2009). There by, trends significance have been investigated under two hypothesis: (1) presence of short-term persistence (STP), and (2) presence of long-term persistence (LTP).

Mann-Kendall Test

Potential trends in each statistic are determined by the Mann-Kendall test (Kendall, 1975; Mann, 1945). Mann–Kendall test is used because it is distribution-free, robust against outliers, and has a higher power for non-normally distributed data (Onoz and Bayazit, 2003; Yue et al., 2002). In addition, it has been used in most previous streamflow trend analyses (Aziz and Burn, 2006; Birsan et al., 2005; Dixon et al., 2006; Lins and Slack, 1999). Mann–Kendall test requires the input data to be serially independent. Many other publications discuss the effects of positive serial correlation in the data structure and the significance of trends (von Storch, 1995; Yue et al., 2002; Hamed and Rao, 1998, Hamed 2008, Kumar et al. 2009).

As a result of Kumar et al. (2009), two techniques from published literatures are adopted in this study. These include Mann–Kendall after trend-free pre-whitening as suggested by Yue et al. (2002) and Mann–Kendall test considering long-term persistence (LTP) as suggested by

Hamed (2008). Trend-free pre-whitening removes only lag-1 autocorrelation; whereas Mann–Kendall test considering LTP considers complete serial correlation structure present in the dataset. Apart from short term persistence as represented by lag-1 autocorrelation, presence of LTP or Hurst phenomenon has been identified as a major source of uncertainty in analyzing hydroclimatic data series (Koutsoyiannis and Montanari, 2007; Cohn and Lins, 2005, Tu et al. 2017).

Presence of LTP behavior in the data series could lead to underestimation of serial correlation in the data structure, and overestimation of significance of Mann–Kendall test (Koutsoyiannis, 2003). To incorporate LTP behavior in the Mann–Kendall test, the technique proposed by Hamed (2008) is used. Thus, overall, two versions of Mann–Kendall test are used in this study: (i) Mann–Kendall with lag-1 autocorrelation and trend-free pre-whitening (MK1), (II) Mann–Kendall with LTP (MK2). These two variations of Mann—Kendall test are used in this study are based on Kumar et al. (2009) incorporation of LTP and serial autocorrelation in relation to statewide streamflow data. Its adoption for the ground water data is described below.

Simple Mann–Kendall test

This is a classical form of Mann–Kendall Test used in many trend studies (Lettenmaier et al., 1994; Lins and Slack, 1999; Dixon et al., 2006) and is used here as a basis for further equations. If $X_1;\ X_2;\ldots;\ X_n$ is the time series of length n, then the Mann–Kendall test statistic S is given by:

$$S = \sum_{i=1}^{n-1}\sum_{j=i+1}^{n} sgn(X_j - X_i) \qquad (2)$$

Where $$sgn(x) = \begin{cases} 1\ for\ x > 0 \\ 0\ for\ x = 0 \\ -1\ for\ x < 0 \end{cases} \qquad (3)$$

The null hypothesis H_0 for the test is "there is no trend in the time series". If H_0 is true then S is normally distributed with

$$E(S) = 0 \quad (4)$$

$$V(S) = \frac{n(n-1)(2n+S)}{18} \quad (5)$$

Where $E(S)$ is the mean and $V(S)$ is the variance of S. Then the Mann—Kendall z is given by:

$$Z = \begin{cases} \frac{S-1}{\sqrt{V(S)}} & for\ S > 0 \\ 0 & for\ S = 0 \\ \frac{S+1}{\sqrt{V(S)}} & for\ x < 0 \end{cases} \quad (6)$$

A positive value of S indicates an increasing trend and vice versa. Test statistic z gives significance level (SL) of rejecting the null hypothesis (chances of rejecting null hypothesis even if there is no trend in the dataset). Confidence level (CL) of rejecting the null hypothesis is given by:

$$CL = 1 - SL \quad (7)$$

Magnitude of trends has been determined using Theil–Sen approach (TSA) (Sen, 1968; Thiel, 1950). The TSA slope β is given by:

$$\beta = median\left[\frac{X_j - X_i}{j-i}\right] \text{ for all } i < j \quad (8)$$

Mann—Kendall test with trend-free pre-whitening (MK1) (appendix 8)

Pre-whitening is a statistical approach to remove the influence of autocorrelation in serial data, such as our groundwater time series data. The trend-free pre-whitening (TFPW) procedure as described by Yue et al. (2002) involves the following steps:

1. Compute the lag-one ($k = 1$) autocorrelation coeffiecient (r_1) using:

$$r_k = \frac{\frac{1}{n-k}\sum_{i=1}^{n-k}(X_i-\bar{X})(X_{i+k}-\bar{X})}{\frac{1}{n}\sum_{i=1}^{n}(X_i-\bar{X})^2} \quad (9)$$

2. If $\frac{-1-1.645\sqrt{n-2}}{n-2}, \leq r_1 \leq \frac{-1+1.645\sqrt{n-2}}{n-2}$, then they are assumed to be serially independent at 10% significance level (CL = 90%) and no pre-whitening is required. Else data are considered to be serially correlated and pre-whitening is required before applying the Mann–Kendall test.
3. Compute non-parametric TSA slope (β) in the sample data by using Eq. (8), and remove the trend from the series to get a detrended series by using the following equation:

$$X_i' = X_i - (\beta * i) \quad (10)$$

4. Compute the lag-1 autocorrelation of the detrended series by using Eq. (9).
5. Remove the lag-one autoregressive component (AR(1)) from the detrended series to get a residual series as given below:

$$y_i' = X_i' - r_1 * X_{i-1}' \quad (11)$$

6. The trend ($\beta * i$) is added back to the residual series to get a blended series:

$$y_i = y_i' + (\beta * i) \quad (12)$$

The Mann–Kendall test is applied to the blended series y_i to determine the significance of the trend. This method has been used to determine trends in streamflow data for several studies (Aziz and Burn, 2006; Birsan et al., 2005; Novotny and Stefan, 2007).

Mann—Kendall test considering LTP (MK2) (appendix 9)

This method is adopted from Hamed (2008), and involves the following steps:

1. Calculation of Hurst coefficient (H):
    a. Time series X_i is detrended using non-parametric TSA slope (Eq. (8)) and the detrended series X_i' is obtained as described in Eq. (10).

b. The equivalent normal variates of rank of the detrended series are obtained using following Eq. (13) below.

$$Z_i = \phi^{-1}\left(\frac{R_i}{n+1}\right) \tag{13}$$

where R_i is the rank of the detrended series X_i', n is the length of the time series, and ϕ^{-1} is the inverse standard normal distribution function (mean = 0, standard deviation = 1).

c. Correlation matrix for a given Hurst coefficient is given by:

$$C_n(H) = \left[\rho_{|j-i|}\right], \qquad \text{for } i = 1:n, j = 1:n \tag{14}$$

$$\rho_l = \frac{1}{2}(|l+1|^{2H} - 2|l|^{2H} + |l-1|^{2H}) \qquad \text{for } l > 1 \tag{15}$$

where ρ_l is the autocorrelation function of lag l for a given H, and is independent of the time scale of aggregation for the time series (Koutsoyiannis, 2003).

d. The value of H is obtained by maximizing the log likelihood function of H as given by Eq. (16).

$$\log L(H) = -\frac{1}{2}\log|C_n(H)| - \frac{Z^T[C_n(H)]^{-1}Z}{2\gamma_0} \tag{16}$$

Where $|C_n(H)|$ is the determinant of correlation matrix $|C_n(H)|$, Z^T is the transpose vector of equivalent normal variates Z (Eq. (13)). $[C_n(H)]^{-1}$ is the inverse matrix, and γ_0 is the variance of Z_i. Equation (16) can be solved numerically for different value of H, and the value for which $\log L(H)$ is the maximum taken as the H value for the given time series X_i. In this study, the value of H is solved between 0.50 and 0.98 with an incremental step of 0.01.

2. Significance level of H is determined (whether obtained value of H in step 1 is significantly different from 0.5 or not) using mean (μH) and standard deviation (σ_H) when H = 0.5 (normal distribution) as given by the following equations:

$$\mu H = 0.5 - 2.87n^{-0.9067} \quad (17)$$

$$\sigma H = 0.77654n^{-0.5} - 0.0062 \quad (18)$$

Equations (17) and (18) are obtained by Hamed (2008). We have used 10% significance level for determining significant H.

3. Calculation of variance: If H is found to be significant the variance of S is calculated using following equation for given H:

$$V(S)^{H\prime} = \sum_{i<j}\sum_{k<l}\frac{2}{\pi}sin^{-2}\left(\frac{\rho|j-i|-\rho|i-l|-\rho|j-k|+\rho|i-k|}{\sqrt{(2-2\rho|i-j|)(2-2\rho|k-l|)}}\right) \quad (19)$$

where ρ_l is calculated from Eq. (15) for given H. Because H is estimated from given data series, $V(S)^{H\prime}$ is a biased estimate. To calculate an unbiased estimate $V(S)^{H\prime}$, the value obtained in Eq. (19) is multiplied by a bias correction factor B.

$$V(S)^{H} = V(S)^{H\prime} \times B \quad (20)$$

where B is a function of H and n. The significance of Mann–Kendall test is computed by using $V(S)^{H}$ in place of $V(S)$in Eq. (6).

The Mann-Kendall test was computed using MATLAB software with code from Kumar et al. (2009).

Autocorrelation Analysis (Appendix 10)

Each groundwater well and PRISM precipitation data were converted from daily data to monthly data and smoothed with a 3-month running mean to reduce intra-seasonal variability. 3-month running mean anomalies are computed by removing the long-term monthly climatology determined from the period of record. Six different focus areas were determined based on the

available data: Floridan aquifer system (FAS), Coastal Plain aquifer system (CPAS), Surficial aquifer system (SAS), Northern aquifer systems (NAS), Combined Statewide aquifer systems (CSAS), and precipitation (PCP).

The autocorrelation analysis involves correlating each 3-month season with the corresponding season's anomalies with values at lags ranging from -24 to +24 months. This study assumes that since the land surface integrates forcing by random weather and climate variability, then the subsurface water conditions will match this reaction; and thereby will provide a red spectrum. It has been shown in the literature that both confined and unconfined aquifers will interact with surface water and climate systems through recharge and discharge (Green et al., 2011, Rakhshandehroo and Amiri 2012, Taylor et al. 2013, Joelson et al. 2016). Therefore, the simplest null hypothesis for groundwater table variability is red noise or a first-order Markov process (Amenu et al. 2005, Chikamoto et al. 2015, Delworth and Manabe 1988, Schlosser and Milly 2002), whose autocorrelation function ρ for a given lag τ is

$$\rho(\tau) = \exp(\frac{-\tau}{\tau_D}) \tag{21}$$

where τ_D is the decorrelation (or e-folding) time scale, also known as groundwater table memory in this study.

Let us suppose $\prod_{y=1,m=1}^{y=n,m=12} X_{y,m}$ is the seasonal anomalies time series (3-month running average) for a given aquifer type where subscript *y* represent year (1 to n), *m* represent season (1 to 12); then the correlation functions are given as below:

$$AC_{m,\delta} = correl\left(\prod_{y=1}^{n} X_{y,m}, \prod_{y=1}^{n} X_{y,m+\delta}\right) \tag{22}$$

where $AC_{m,\delta}$ is autocorrelations for season *m*, and at lead/lag δ which ranges from -24 to +24. *Correl* is the linear correlation coefficient between the two series. For

$\delta \geq 12, X_{y,m+\delta} = X_{y+1,m+\delta-12}$, and $\delta \leq 12, X_{y,m+\delta} = X_{y-1,m+\delta+12}$. The t-statistic for the regression coefficient was determined and converted into the statistical probabilities (p-value). Thus, every year contributes one sample in the given time series, (e.g. $\prod \frac{n}{y=1} X_{y,m}$) for computing correlation. We determined degrees of freedom by accounting for serial autocorrelation in the time series and accordingly reducing the effective sample size using the NCL function equiv_sample_size (NCL, 2018).

All autocorrelation work was done in NCL using code based on Kumar et al. (2019) and is located in appendix 11.

Chapter 4: Results

Trends in Ground Water

The trends in the well data are analyzed by performing the Mann-Kendall trend analysis for annual groundwater statistics following the methods from the previous chapter. The annual Mann—Kendall Z values ($z \geq 1.96$ and $z \leq -1.96$ are statistically significant) for all wells and the statewide averages are presented in Table 2. Z values for each aquifer and the statewide averages are presented in Table 3. The total number of stations showing significant trend (>95% confidence interval) for short-term and long-term Mann—Kendall tests are presented in Table 4.

Annual average, minimum, maximum, 7-day minimum, 7-day maximum, and range trends are calculated for each groundwater monitoring well. Each statistic is further classified based on the aquifer system that the well screen is located in for each well. The SAS and NAS show no significant trend for any of the statistics tested when considering both STP and LTP. The FAS shows significant declines in annual average, minimum, and 7-day minimum when STP is considered and loses significance in only 7-day minimum when LTP is considered. The CPAS shows statistically significant declines in all statistics tested for both STP and LTP with the exception of annual range which shows significant increased for both STP and LTP.

Large percentages of streamflow stations (75% or more) have been shown previously to lose statistical significance as LTP is considered for Mann-Kendall tests (Kumar et al. 2009). In the contrary, our study indicates that none of the test statistics show this large decrease in wells showing statistical significance when LTP is incorporated. Annual average water table showed the largest decrease in Z value when incorporating LTP with around 50% of the wells losing significance. Annual minimum, 7 day minimum, and 7 day maximum all show a large percentage of wells with significant Z values (66-75%) and all show a large decrease when LTP is considered

(38-48%). Overall, all statistics considered show a large percentage of wells exhibiting mostly significant decreasing trends (down-pointing triangles in Figures 4 and 5) except for the "range" (between minimum and maximum level), which show increasing trends.

Table 2. Mann—Kendall "Z value" for annual groundwater statistics using MK1/MK2. Z value for the stations showing significant trends at 95% confidence level ($z \geq 1.96$ and $z \leq -1.96$) are shown in bold (Aq.: Aquifer, M_1: Average, L1: 1-day minimum water table, L7: 7-day minimum water table, H1: 1-day maximum water table, H7: 7-day maximum water table).

Well ID	Aq	M_1	Range	L1	L7	H1	H7
304942082213801	FAS	**-2.73**/-1.04	1.77/1.77	-1.63/-0.69	**-3.20**/-1.45	-1.82/-0.74	**-3.15**/-1.35
304949083165301	FAS	1.40/0.66	0.85/0.85	**2.26**/1.02	0.77/0.77	**2.03**/0.96	1.19/1.19
305356084534601	FAS	-0.01/-0.01	1.35/0.66	0.51/0.51	**-2.31**/**-2.31**	0.61/0.61	**-2.34/-2.34**
305736084355801	FAS	-1.66/-1.66	-0.51/-0.51	-1.32/-1.32	-1.53/-1.53	-1.14/-1.14	-1.45/-1.45
310507084262201	FAS	-1.61/-1.61	-0.80/-0.80	-1.14/-1.14	-1.58/-0.81	-1.09/-1.09	-1.45/-0.76
310651084404501	FAS	-1.45/-0.67	0.41/0.41	-0.67/-0.67	**-2.24**/-0.96	-0.14/-0.14	-1.48/-0.67
310706082155101	FAS	**-4.51/-1.99**	**2.43/2.43**	**-3.28**/-1.48	**-5.04/-5.04**	**-3.18**/-1.43	**-4.98/-4.98**
310813083260301	FAS	**-7.15/-2.36**	**2.52/2.52**	**-6.92/-2.76**	**-6.89/-3.53**	**-6.97/-2.78**	**-6.97/-6.97**
310818081294201	FAS	**4.28**/1.31	-0.04/-0.04	**4.25**/1.50	**4.38**/1.41	**3.81**/1.25	**4.41**/1.38
311007081301702	FAS	**6.74/1.97**	**-2.35/-2.35**	**6.32**/1.89	**6.47/2.08**	**6.19/2.47**	**6.37/2.05**
311009084495503	SA	-1.52/-1.52	**1.99/1.99**	-0.24/-0.24	-1.94/-1.94	0.39/0.18	-1.74/-0.83
311802084192301	CPAS	**-2.76**/-1.28	0.00/0.00	**-2.08/-2.08**	**-3.94**/-1.73	**-2.16/-2.16**	**-4.04**/-1.82
311802084192302	FAS	-1.48/-1.48	-1.74/-1.74	-1.56/-1.56	-1.11/-1.11	-1.19/-1.19	-1.63/-1.63
312127084065801	FAS	**-3.91**/-1.35	-0.30/-0.30	**-3.07**/-1.17	**-4.43**/-1.43	**-2.92**/-1.11	**-4.28**/-1.37
312232084391701	FAS	-1.09/-0.45	**2.08/2.08**	**2.45**/0.93	-1.63/-0.76	1.87/0.66	-1.90/-0.88
312617084110701	FAS	**-2.89/-2.89**	-1.83/-0.96	**-2.31**/-1.07	**-2.97**/-1.48	-1.39/-1.39	**-2.81**/-1.37
312712082593301	FAS	**-7.76/-3.09**	**3.54/3.54**	**-8.10/-2.42**	**-7.34/-7.34**	**-8.04/-2.41**	**-7.44/-7.44**
312919084153801	FAS	-0.25/-0.11	1.45/1.45	0.21/0.10	-0.98/-0.43	0.27/0.14	-0.85/-0.40
313146083491601	FAS	**-8.46/-2.66**	-0.09/-0.09	**-8.31/-2.80**	**-8.12/-3.49**	**-8.25/-2.78**	**-8.15/-3.59**
313532084203501	CPAS	**-6.19/-2.04**	**2.05/2.05**	**-6.53/-2.31**	**-4.88/-2.50**	**-6.55/-2.32**	**-4.93/-2.46**
313554084062501	CPAS	**2.66**/0.83	0.68/0.68	**3.44**/1.34	1.63/0.61	**3.57**/1.39	1.56/0.56
313701081543501	FAS	**-5.79**/-1.86	**4.07**/1.58	**-3.47**/-1.11	**-5.82/-2.06**	**-3.20**/-0.91	**-5.79/-2.05**
313808084093601	FAS	-0.27/-0.11	1.12/0.56	0.14/0.06	-0.95/-0.95	-0.20/-0.08	-1.56/-1.56
313845081361701	FAS	**-4.64**/-1.39	**3.05/3.05**	**-3.39**/-0.99	**-4.80**/-1.54	**-3.15**/-0.97	**-4.75**/-1.53
314330084005402	FAS	-1.77/-1.77	**2.00/2.00**	**-2.50**/-1.28	**-2.08/-2.08**	**-3.15**/-1.29	**-2.60/-2.60**
314330084005403	SA	0.13/0.13	0.89/0.89	0.47/0.47	-0.64/-0.33	0.58/0.58	0.09/0.04
314602084473701	CPAS	**-7.00**/-1.95	-0.93/-0.93	**-6.84**/-1.86	**-6.26/-2.32**	**-6.92**/-1.84	**-6.00/-2.40**
315950081161201	SA	0.80/0.38	**-3.86/-3.86**	**-2.21/-2.21**	**3.49**/1.58	-1.19/-1.19	**4.04**/1.87
320122080510204	FAS	**4.67**/1.21	0.13/0.13	**4.98**/1.26	**3.57**/1.07	**5.11**/1.33	**3.57**/1.07

320202080541201	FAS	**5.87**/1.56	0.12/0.12	**6.06**/1.61	**4.90**/1.50	**5.98**/1.55	**4.80**/1.47
320226082301101	FAS	**-7.49/-2.47**	**4.07/4.07**	**-7.28/-2.77**	**-7.05/-2.62**	**-7.23/-2.75**	**-7.08/-2.63**
320433081042701	FAS	**7.26/2.17**	**-2.26/-2.26**	**7.47/2.13**	**6.84/2.25**	**7.36/2.00**	**6.94/2.18**
321302082243601	FAS	**-7.60/-2.27**	**3.96/3.96**	**-7.52/-2.60**	**-7.00/-3.41**	**-7.55/-2.61**	**-7.10/-3.29**
322036084590301	CPAS	**-8.33/-2.01**	1.22/0.59	-8.12/-1.**96**	**-8.12/-2.01**	**-8.10/-1.96**	**-8.12/-2.01**
322245083290101	CPAS	**-8.10/-2.00**	**4.49/4.49**	**-7.70/-2.00**	**-7.86/-2.04**	**-7.39/-1.96**	**-7.99/-2.03**
322652083033001	FAS	**-3.57/-3.57**	0.07/0.07	**-3.34/-3.34**	**-3.73/-3.73**	**-3.18/-3.18**	**-3.81/-3.81**
323030083030003	SCP	**-8.38/-2.39**	**4.38/4.38**	**-8.28/-2.36**	**-8.07/-2.59**	**-8.25/-2.41**	**-8.10/-2.67**
323302083263401	SCP	**-6.97**/-1.85	**3.94/3.94**	**-6.87**/-1.83	**-6.71/-2.06**	**-6.84**/-1.82	**-6.68/-2.05**
325232082131501	SCP	**-8.46**/-1.95	**5.48/2.08**	**-8.25/-1.99**	**-8.33**/-1.92	**-8.25/-1.99**	**-8.33**/-1.92
331711081573701	SCP	**-6.76**/-1.93	1.11/1.11	**-6.84/-2.00**	**-7.10/-2.03**	**-6.76/-2.02**	**-7.00/-2.05**
334207084254801	NAS	1.22/0.36	1.09/1.09	1.03/0.32	0.35/0.11	1.40/0.41	0.09/0.03
335517084164001	NAS	**-6.16/-2.46**	**3.57/3.57**	**-4.70/-2.17**	**-6.24/-3.28**	**-4.85/-2.42**	**-5.85/-5.85**
345403085160001	NAS	**3.49**/1.66	**-2.97/-2.97**	**2.05/2.05**	**3.83**/1.61	1.45/1.45	**3.99**/1.55
Statewide Average		**-3.70**/-1.63	**2.16/2.16**	**-4.04**/-1.87	**-3.28**/-1.48	**-3.44**/-1.72	**-3.28**/-1.48

Table 3. Average "Z value" for annual groundwater statistics using MK1/MK2 separated by aquifer. Z value for the stations showing significant trends at 95% confidence level ($z \geq 1.96$ and $z \leq -1.96$) are shown in bold. P-scores are shown as asterisks (*) beside the Z value (*: 95% confidence, **: 99% confidence, ***: 99.9% confidence). (M_1: Average, L1: 1-day minimum water table, L7: 7-day minimum water table, H1: 1-day maximum water table, H7: 7-day maximum water table).

Z-Values	M_1	Range	L1	L7	H1	H7
FAS	**-2.89****/-1.30	1.87/1.87	**-3.31*****/**-3.31*****	**-3.31*****/-1.70*	-1.92*/-0.98	-1.74*/-0.79
CPAS	**-7.10*****/**-2.34****	**3.02/3.02**	**-7.08*****/**-2.76****	**-7.00*****/**-2.73****	**-6.89*****/**-2.56****	**-6.89*****/**-2.56****
SA	-0.33/-0.33	-0.20/-0.10	0.04/0.04	0.72/0.31	-0.85/-0.85	0.01/0.01
NAS	-1.45/-0.57	0.51/0.51	-1.32/-0.58	-1.48/-0.68	-1.03/-0.40	-1.58/-0.53
SAS	**-3.70*****/-1.63	**2.16/2.16**	**-4.04****/-1.87*	**-3.28*****/-1.48	**-3.44*****/-1.72*	**-3.28*****/-1.48

Table 4. Number of wells showing significant trends (95% confidence level) for annual statistics using MK1/MK2 (total number of wells = 43). Values for each row should be read as (MK1(+/-) / MK2(+/)). (M_1: Average, L1: 1-day minimum water table, L7: 7-day minimum water table, H1: 1-day maximum water table, H7: 7-day maximum water table).

Total	M_1	Range	L1	L7	H1	H7
FAS	(5/2)/(11/8)	(9/8)/(3/3)	(6/2)/(14/10)	(6/2)/(13/10)	(7/1)/(13/7)	(6/2)/(11/6)
CPAS	(1/0)/(9/4)	(5/5)/(0/0)	(0/0)/(9/7)	(0/0)/(9/7)	(1/0)/(9/7)	(1/0)/(9/6)
SA	(0/0)/(0/0)	(0/1)/(0/1)	(1/0)/(0/0)	(1/0)/(0/0)	(0/0)/(1/1)	(0/0)/(0/0)
NAS	(1/0)/(1/1)	(0/1)/(1/1)	(1/0)/(1/1)	(1/0)/(1/1)	(1/1)/(1/1)	(0/0)/(1/1)
SAS	(7/2)/(21/13)	(16/15)/(5/5)	(8/2)/(24/18)	(8/2)/(23/18)	(9/2)/(24/16)	(7/2)/(21/13)

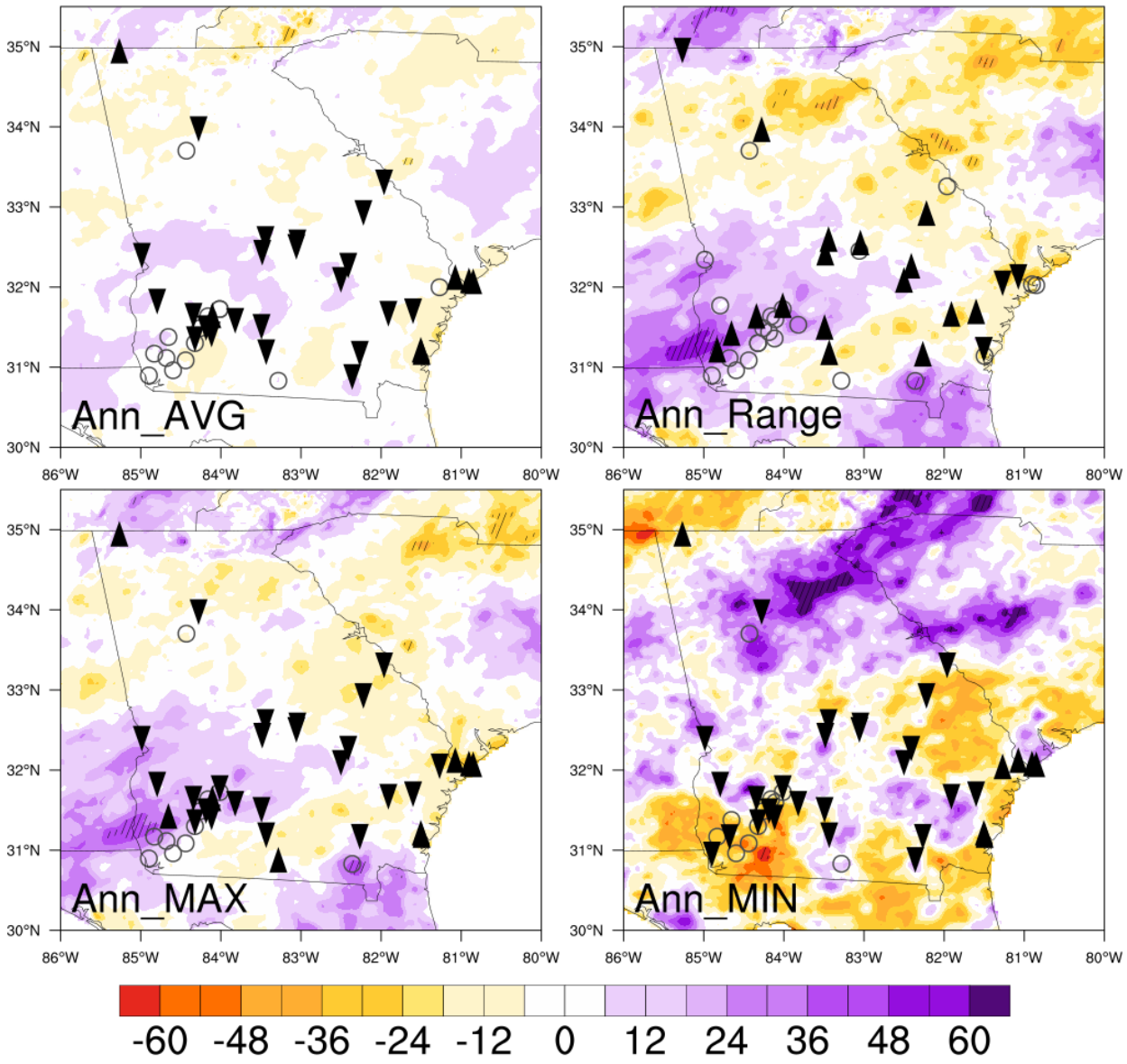

Figure 4. Spatial distribution of wells showing significant trends using MK1. (Ann_AVG: Annual Average, Ann_Range: Annual Range, Ann_MAX: Annual 1-day Maximum, Ann_MIN: Annual 1-day Minimum). The background color for the map shows linear trend for annual precipitation in units of % change in 37 years (1981 to 2017) and the corresponding statistics from monthly PRISM climate data. Hatching signifies statistical significance linear regression based trend. Statistical significance (hatching) in precipitation is sparse across the state and typically cover less than 5% area hence not statistically significant. Black up-pointing and down-pointing triangles show increasing and decreasing trends of groundwater level based on Mann-Kendall test (MK1), respectively. Open circles show streamflow stations with no significant trends.

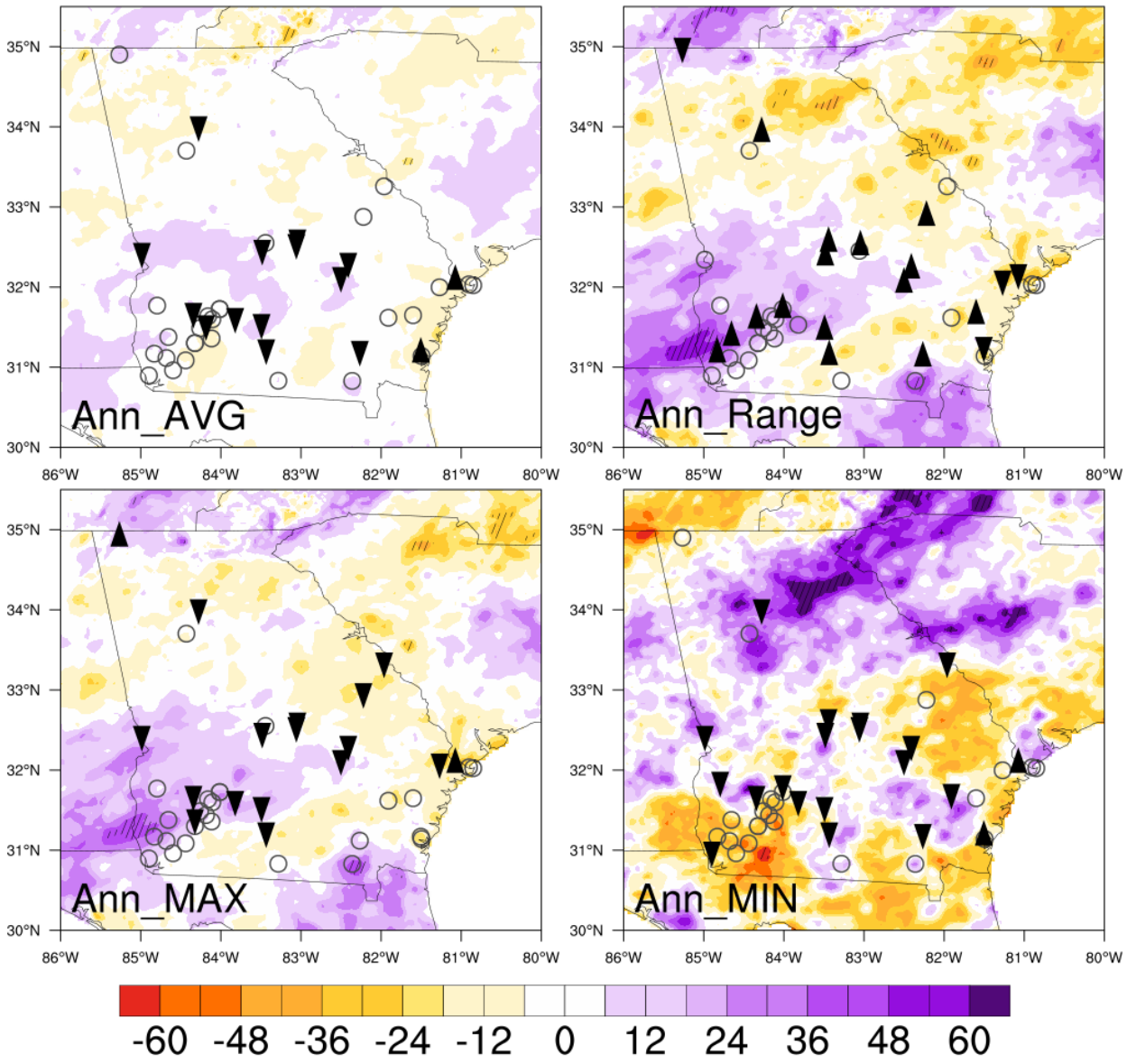

Figure 5. Spatial distribution of wells showing significant trends using MK2. (Ann_AVG: Annual Average, Ann_Range: Annual Range, Ann_MAX: Annual 1-day Maximum, Ann_MIN: Annual 1-day Minimum) The background color for the map shows linear trend for annual precipitation in units of % change in 37 years (1981 to 2017) and the corresponding statistics from monthly PRISM climate data. Hatching signifies statistical significance linear regression based trend. Statistical significance (hatching) in precipitation is sparse across the state and typically cover less than 5% area hence not statistically significant. Black up-pointing and down-pointing triangles show increasing and decreasing trends of groundwater level based on Mann-Kendall test (MK2), respectively. Open circles show streamflow stations with no significant trends.

Climate Trends (Precipitation and Temperature)

To investigate if groundwater trends are related to climatic factors, Mann-Kendall analysis has also been performed for annual precipitation, temperature, and streamflow for the years 1981 to 2017 across Georgia. Precipitation and temperature trends are calculated based on 43 PRISM 4km X 4km grid that is nearest to each of the 43 monitoring wells, respectively.

Precipitation trend (see color maps in Figures 6 and 7) has very little or no significance statewide. Similarly, temperature shows very little significant in daytime temperatures and slightly more with nighttime temperatures with STP. Average temperature shows some significance but is only considering linear trend.

Streamflow Trends

Streamflow has been calculated based on 33 streamflow stations. Overall precipitation streamflow (Figure 6 and 7) show less statistical significance (short and long term) when compared to groundwater level trends (Fig. 4 and 5). Streamflow has 13 stations showing significant decreasing minimum baseflow (Fig. 6 and 7), but only three stations with significantly decreasing minimum baseflow when LTP is considered. The other statistics for streamflow show no significant values

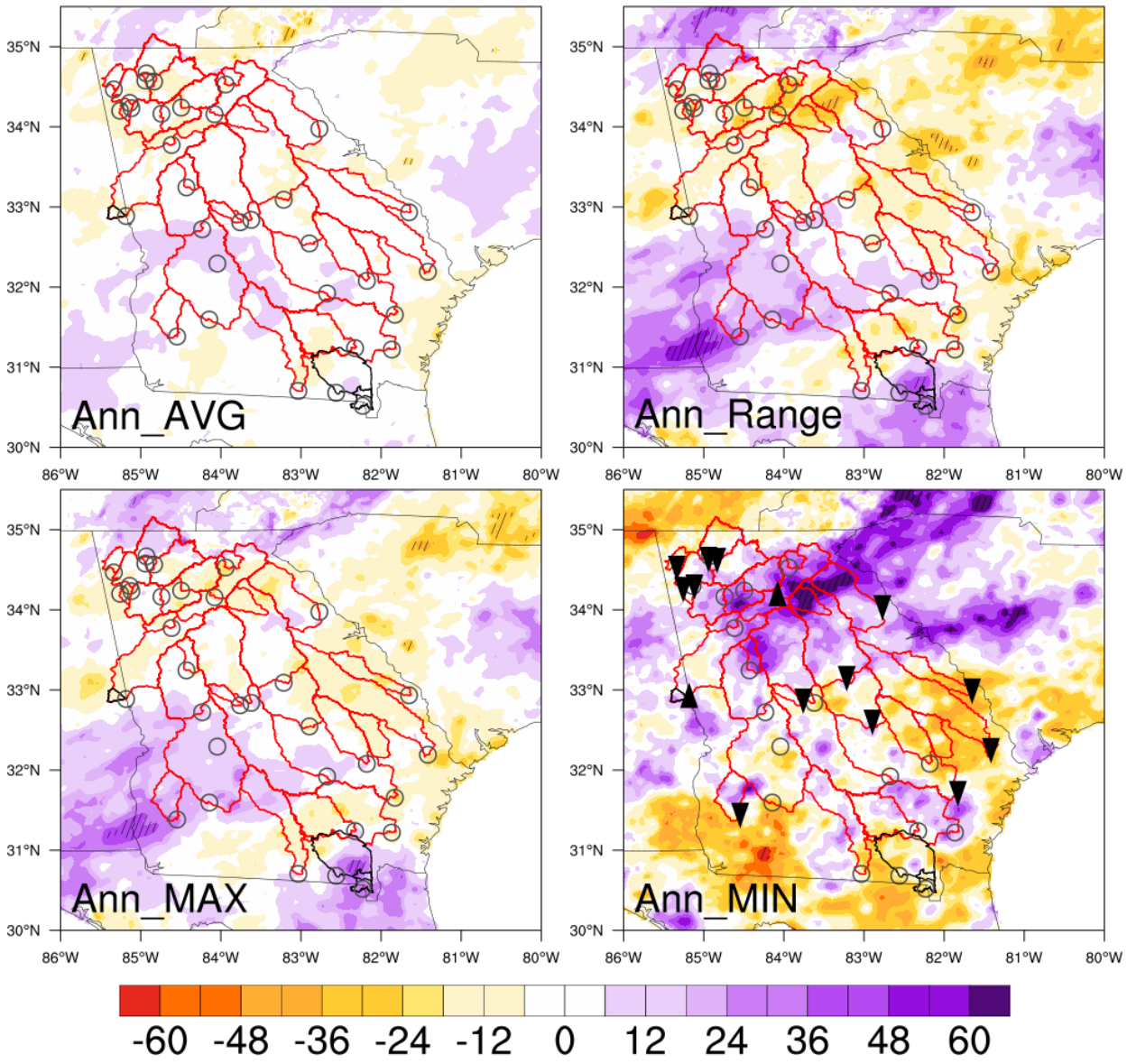

Figure 6. Spatial distribution of stream gauging stations showing significant trends using MK1. (Ann_AVG: Annual Average, Ann_Range: Annual Range, Ann_MAX: Annual 1-day Maximum, Ann_MIN: Annual 1-day Minimum). Black and red lines indicate watershed boundaries. The background color for the map shows linear trend for annual precipitation in units of % change in 37 years (1981 to 2017) and the corresponding statistics from monthly PRISM climate data. Hatching signifies statistical significance linear regression based trend. Statistical significance (hatching) in precipitation is sparse across the state and typically cover less than 5% area hence not statistically significant. Black up-pointing and down-pointing triangles show increasing and decreasing trends of streamflow based on Mann-Kendall test (MK2), respectively. Open circles show streamflow stations with no significant trends

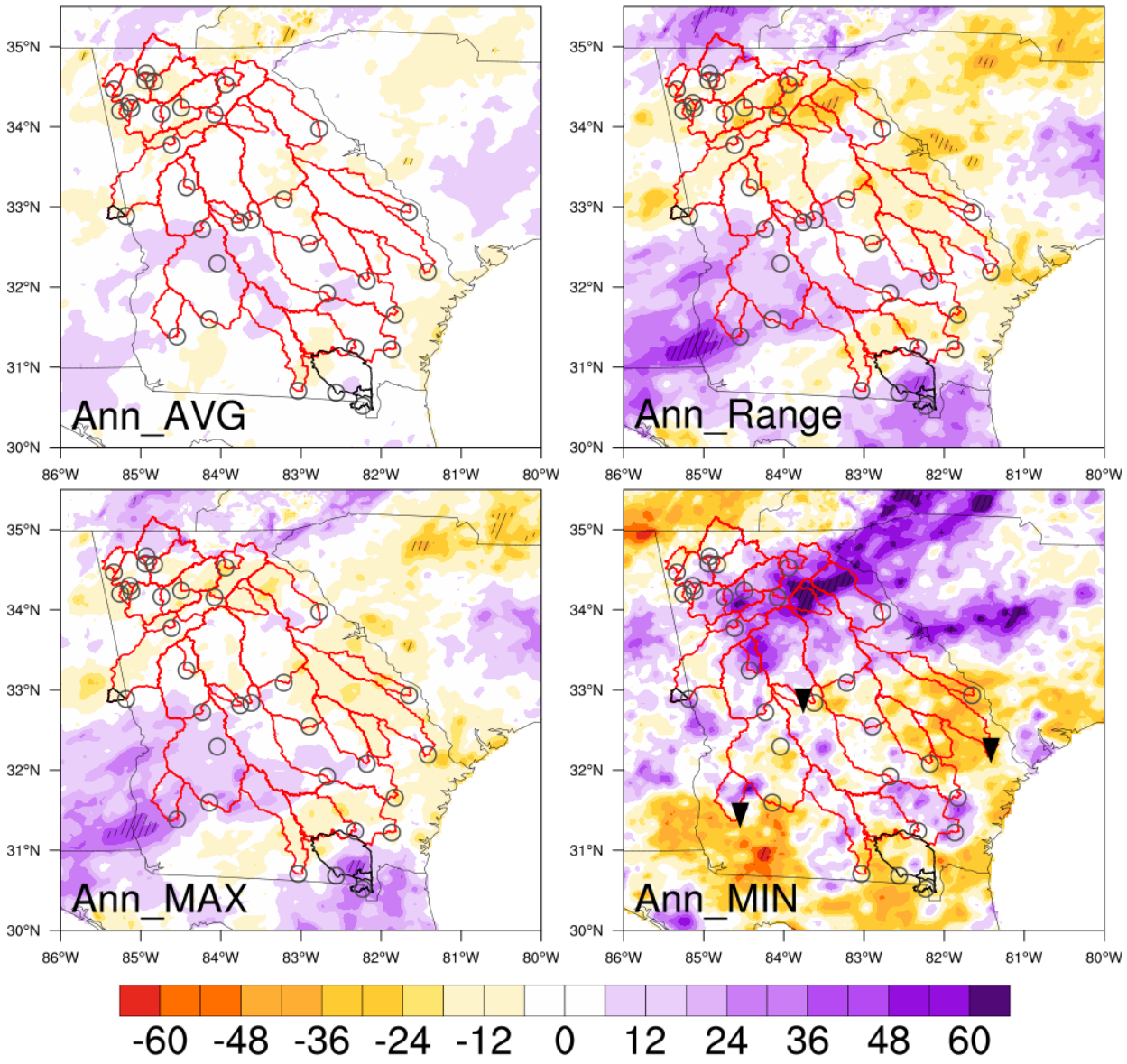

Figure 7. Spatial distribution of stream gauging stations showing significant trends using MK2. (Ann_AVG: Annual Average, Ann_Range: Annual Range, Ann_MAX: Annual 1-day Maximum, Ann_MIN: Annual 1-day Minimum). Black and red lines indicate watershed boundaries. The background color for the map shows linear trend for annual precipitation in units of % change in 37 years (1981 to 2017) and the corresponding statistics from monthly PRISM climate data. Hatching signifies statistical significance linear regression based trend. Statistical significance (hatching) in precipitation is sparse across the state and typically cover less than 5% area hence not statistically significant. Black up-pointing and down-pointing triangles show increasing and decreasing trends of streamflow based on Mann-Kendall test (MK2), respectively. Open circles show streamflow stations with no significant trends

Drivers of Ground Water Trends

Annual time series of standardized departures and its seasonality for the 43 analyzed wells are presented in Figure 8. The annual trend shows most of the wells following along similar decreasing trends except for 6 wells (well 9, 10, 29, 30, 32, and 34). Out of 37 stations that show decreasing tendencies, 20 stations found to be statistically significant based on MK1 and 12 stations were found to be statistically significant based on MK2 test. The 6 wells that differ from these show an overall increasing tendency for the 37 years out of which 6/3 (MK1/MK2) are significant. Five of the increasing tendency wells are located along the Atlantic coast of Georgia and begin the record with substantially negative water table elevations in 1981. These wells have been reported to be near former municipal pumping locations and the increase in water table may be due to ceases of pumping and natural recharge (GADNR, 2006). The last increasing well is located in southwestern Georgia near a Super Fund site.

The seasonal cycle plot standardized anomalies for all wells and averaged over 37 years for each day of the year. The groundwater shows a strong seasonality with a wet period corresponding to spring (March-May) and a dry season corresponding to summer (June-August). Fall through winter months (September-February) show a general increasing trend back to the wet season. The seasonal time series plot shows periods of maximum water table (typically spring) and minimum water table (typically summer).

Figure 9 show annual averages standardized anomalies averaged across different wells each of the 4 aquifer systems together as well as the state wide average. Individual aquifer averages were determined for the Floridan aquifer (FAS) that has 27 number of wells, Coastal Plain aquifer system (CPAS) having 10 wells, surficial aquifer system (SA) 3 wells, and the Northern aquifer

systems (NAS), having 3 wells. P-values have been calculated for each time series and are presented in Table 3.

The SA and the NAS each have the least number of wells (3 each) and show a similar neutral trend over the 37 years. Since there is no notable change in precipitation trend over the monitoring period, this aquifer response is expected. P-value statistics confirm this hypothesis since no statistics for either of these aquifer systems show P-values of 0.05 or less. The statewide average groundwater table is largely influenced by the FAS due to the large amount of monitoring wells in the aquifer (27 of the 43). The FAS time series shows a slightly decreasing trend over the 37 years with periods of large fluctuations (variability). The state wide decreasing trend is statistically significant for MK1 across all statistics, but only shows significance when MK2 is considered with range.

The FAS is hydrologically interconnected with surface water bodies and may act either as an unconfined or a confined aquifer depending on location. Therefore, the similarity in trends between the surficial aquifer and the FAS is expected. Likewise, the FAS shows similarities to the deeper, mostly confined CPAS. Floridian and statewide aquifer statistics show very similar trends in P-value with annual average, minimum, and 7-day minimum all showing significant P-value for STP. Statewide also shows significant P-value for annual maximum and 7-day maximum STP water table levels.

The confined CPAS by far shows the largest decreasing trend of any aquifer systems in the state and lacks large fluctuations likely caused by ENSO and other climatic variability. This may reflect the much longer residence time and mixing processes in the deeper aquifers. P-values also confirm this trend which all statistics showing statistically significant values except for range which shows an inverse trend. The CPAS is also the only aquifer that is unaffected across all

statistics when LTP is considered. The time series analysis and the significant P-value reveal that climate—groundwater interactions do not readily explain the decreasing trend in groundwater in the FAS and CPAS.

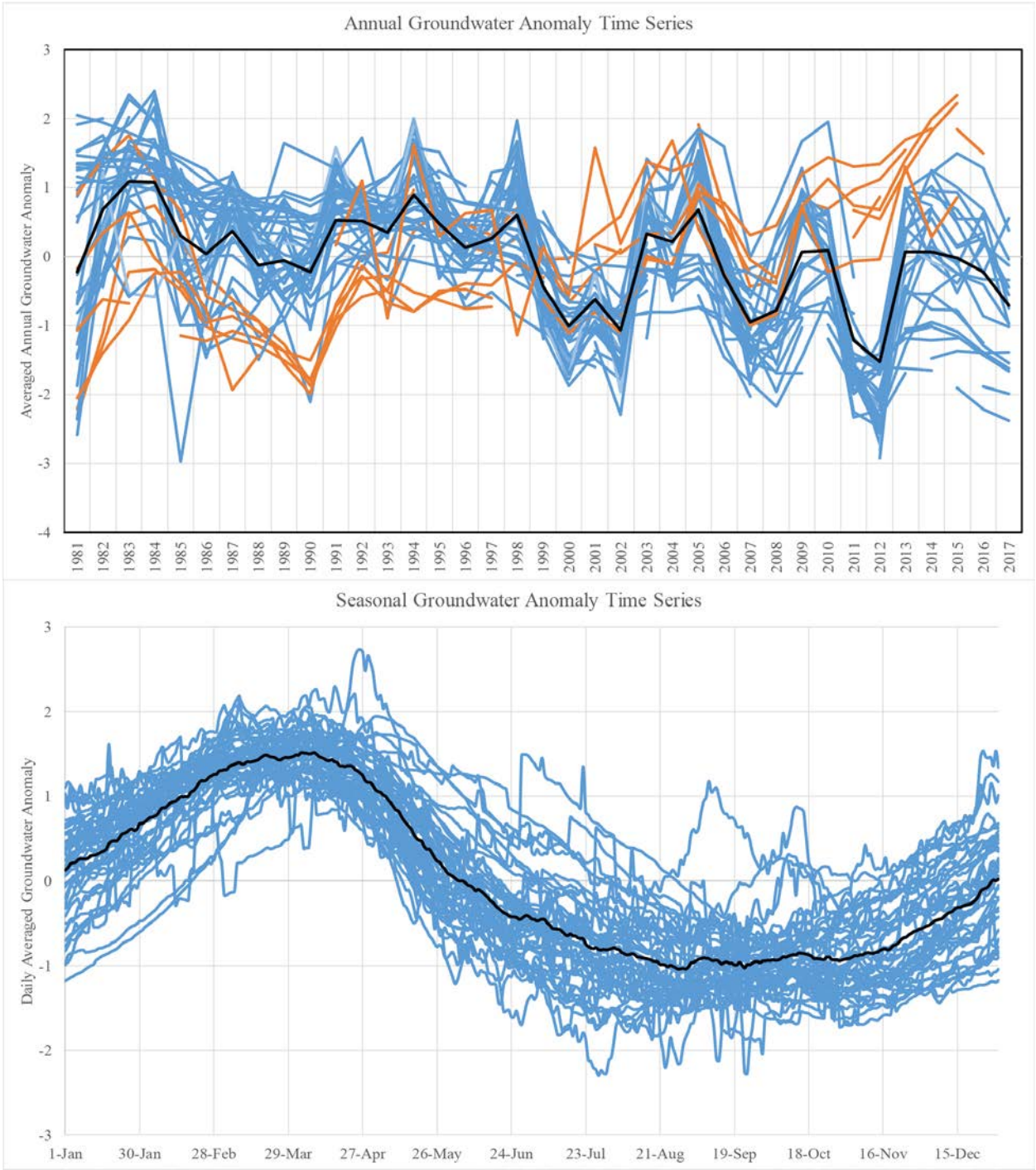

Figure 8. Diagram on top is the annual groundwater time series for all 43 wells analyzed in the study. Most wells show overall decreasing trends showing in blue and 6 wells showing increasing trends shown in orange (9, 10, 29, 30, 32, and 34). The bottom diagram is the average daily water table for each well to show seasonality in the groundwater. The wells show strong seasonality with a wet season in the spring and a dry season in the summer. Statewide average for both graphs is shown in black.

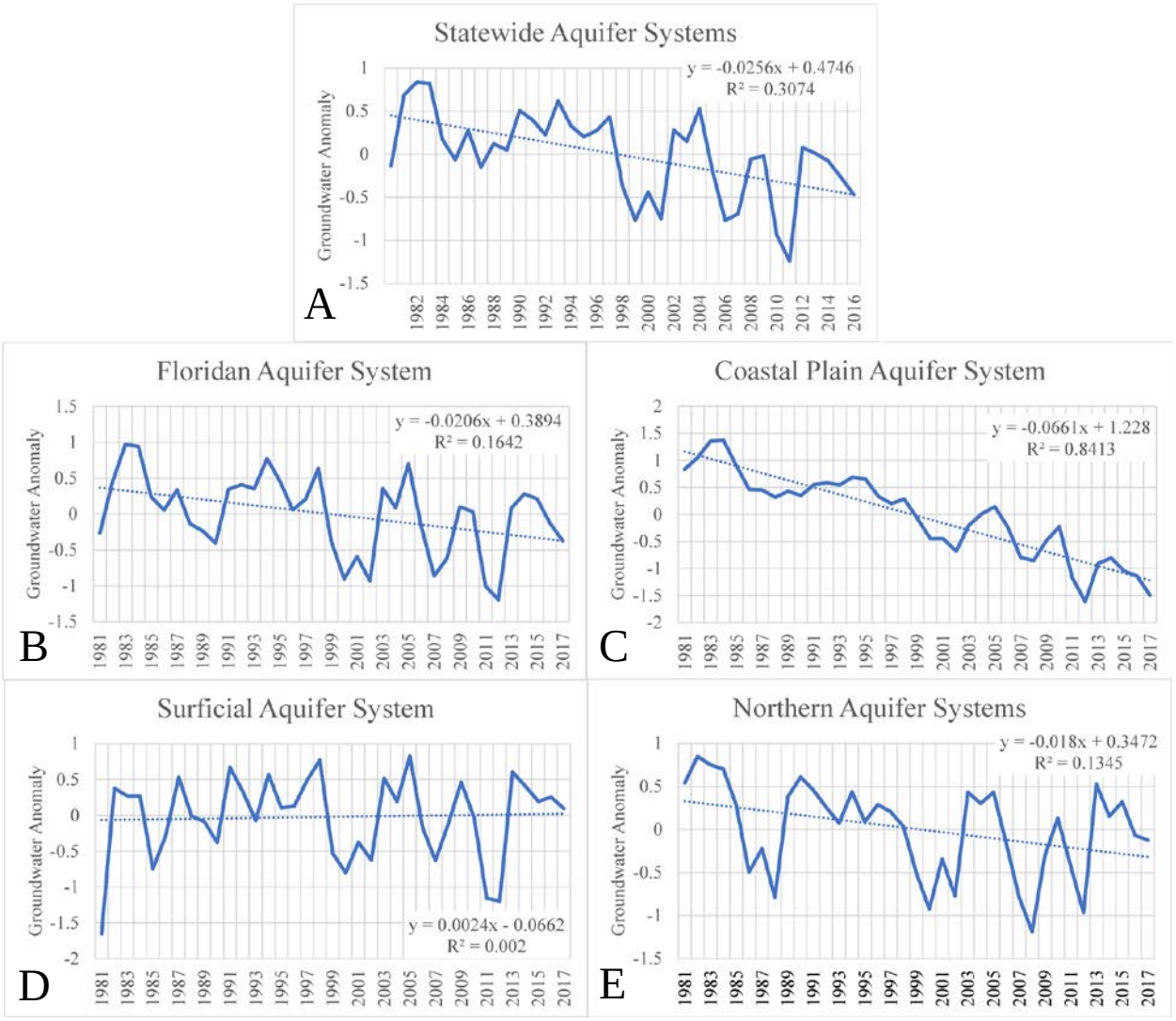

Figure 9. Collage of graphs showing trends of water table elevation in different aquifers in Georgia. Linear trend lien for each time series, linear equation, and R^2 are included in each graph. (A) Shows the statewide time series of average for all four aquifers. (B) Shows the Floridan aquifer system. The Floridan aquifer system has the largest quantity of monitoring wells (27), so the statewide average looks similar due to the large number of wells in the Floridan. (C) Shows the Coastal Plain aquifer system. The Coastal Plain aquifer system has the greatest amount of decrease amongst all the aquifers. (D) Shows the surficial aquifer system. The surficial aquifer shows the least amount of change over the monitoring period. (E) Shows the Northern aquifer systems. The northern aquifer systems show large fluctuations but remains mostly neutral over the time series in terms of average water table level.

Time series analysis attempts to determine any climatic forcings that may lead to groundwater decrease across Georgia as a result. El Nino and La Nina have previously been shown to cause fluctuations in groundwater of the Upper Floridan aquifer in southwestern Georgia (Singh et al., 2015; Singh et al., 2016; Mitra et al., 2014). Statewide annual groundwater level anomalies for each individual aquifer compared to precipitation at the same location as the well is presented in Figure 10. Statewide annual groundwater level anomalies for each individual aquifer compared to ENSO in is presented in Figure 11.

A correlation analysis was performed for groundwater table anomaly, precipitation anomaly, and ENSO anomaly and is presented in Table 5. The analysis determines the correlation between the groundwater anomaly and precipitation anomaly, groundwater anomaly and ENSO anomaly, and precipitation anomaly and ENSO anomaly considering all 37 years of data. The correlation analysis shows a relatively low correlation between the statewide water table and ENSO. The correlation was also analyzed for average of individual aquifer. The Floridan, Coastal Plain, surficial, and northern aquifers were analyzed. The surficial aquifer shows the highest correlations of all the aquifers between all three analyses. On average, the shallower aquifers showed the most correlation with precipitation and ENSO while the deeper aquifers showed the least correlation with climate. Interestingly, all aquifers showed more correlation to precipitation than precipitation did to ENSO. The ENSO—groundwater relationship has been shown to be present in the surface water and shallow aquifers in previous studies (Singh et al., 2015; Singh et al., 2016; Mitra et al., 2014). The correlation analysis also shows that the Coastal Plain aquifer,

the deepest aquifer system, has the lowest correlation, or the poorest connection to climate variables corresponding with previous studies (see references above).

Table 5. Correlation Analysis for Georgia groundwater table anomaly precipitation anomaly, and ENSO anomaly. Statistically significant values are in bold. P-scores are shown as asterisks (*) beside the correlation (*: 95% confidence, **: 99% confidence, ***: 99.9% confidence).

Aquifer	Groundwater/Precipitation	Groundwater/ENSO	Precipitation/ENSO
State Average	**0.58*** **	**0.38***	**0.50****
Floridan Aquifer	**0.66*** **	**0.40***	**0.48****
Coastal Plain Aquifer	0.18	0.09	**0.45****
Surficial Aquifer	**0.75*** **	**0.47****	**0.51****
Northern Aquifers	**0.58*** **	**0.37***	**0.41***

Time series comparisons have also been conducted between groundwater anomaly data and NASA's GRACE total water storage anomalies data (Figure 12). The GRACE project accurately measured variations in Earth's gravity field, which partly correlate to regional changes in groundwater storage on Earth's surface, among other factors. GRACE data show a very similar trend to groundwater throughout the comparative time periods. The results show that the regional gravity average increases with rising water table or groundwater storage. Agreement between the data and GRACE data indicates that the analysis is consistent with other independent water balance metrics.

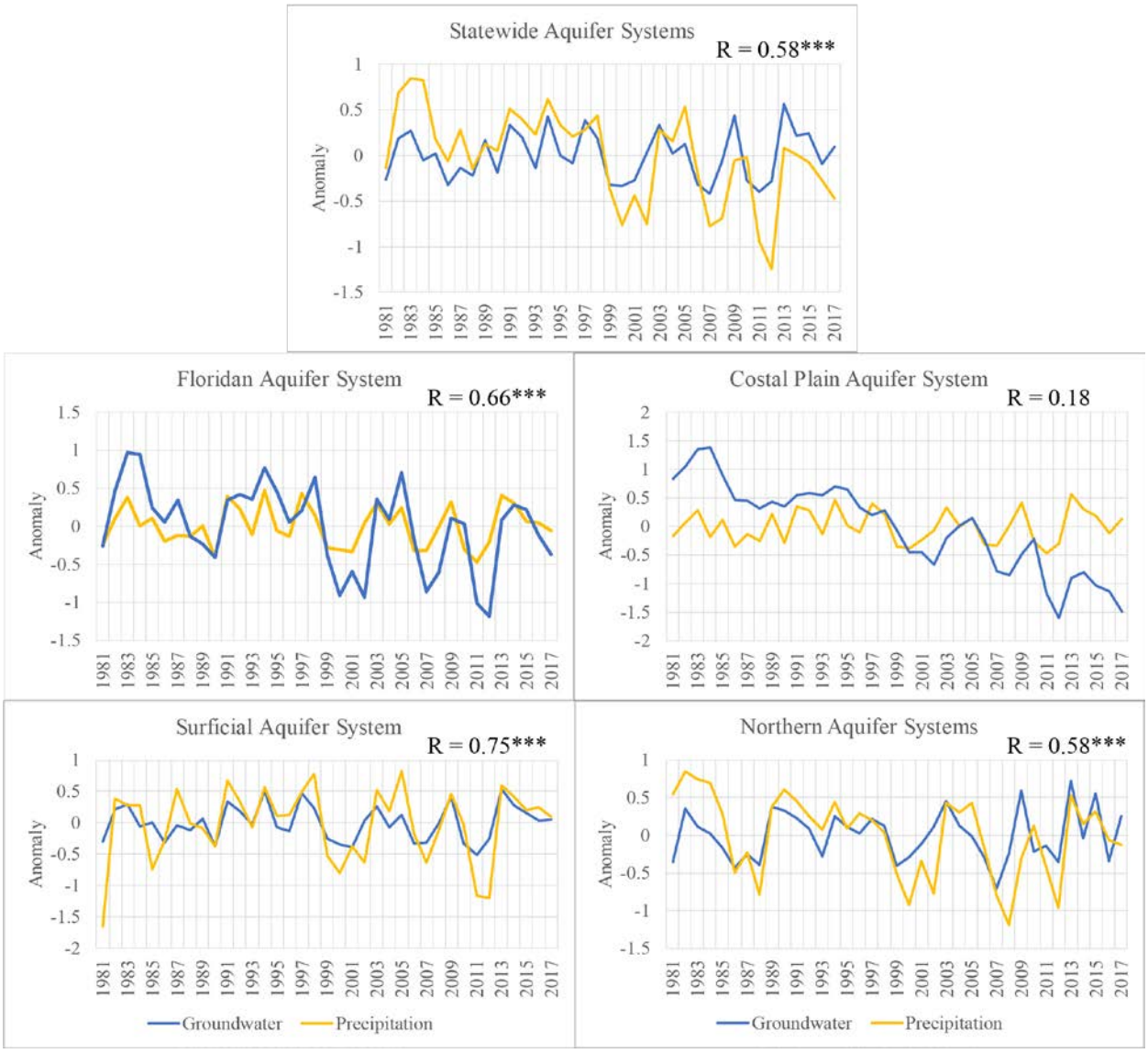

Figure 10. Graph shows annual Georgia groundwater table anomaly (blue) and precipitation anomaly (gold). The two trends show similar increasing and decreasing trends with a slight time lag between precipitation and groundwater fluctuations. Correlation (R) for each set of time series is added to the top right of the chart. P-scores are shown as asterisks (*) beside the R value (*: 95% confidence, **: 99% confidence, ***: 99.9% confidence). A) Shows the statewide time series of average for all four aquifers. (B) Shows the Floridan aquifer system. (C) Shows the Coastal Plain aquifer system. (D) Shows the surficial aquifer system. (E) Shows the Northern aquifer systems.

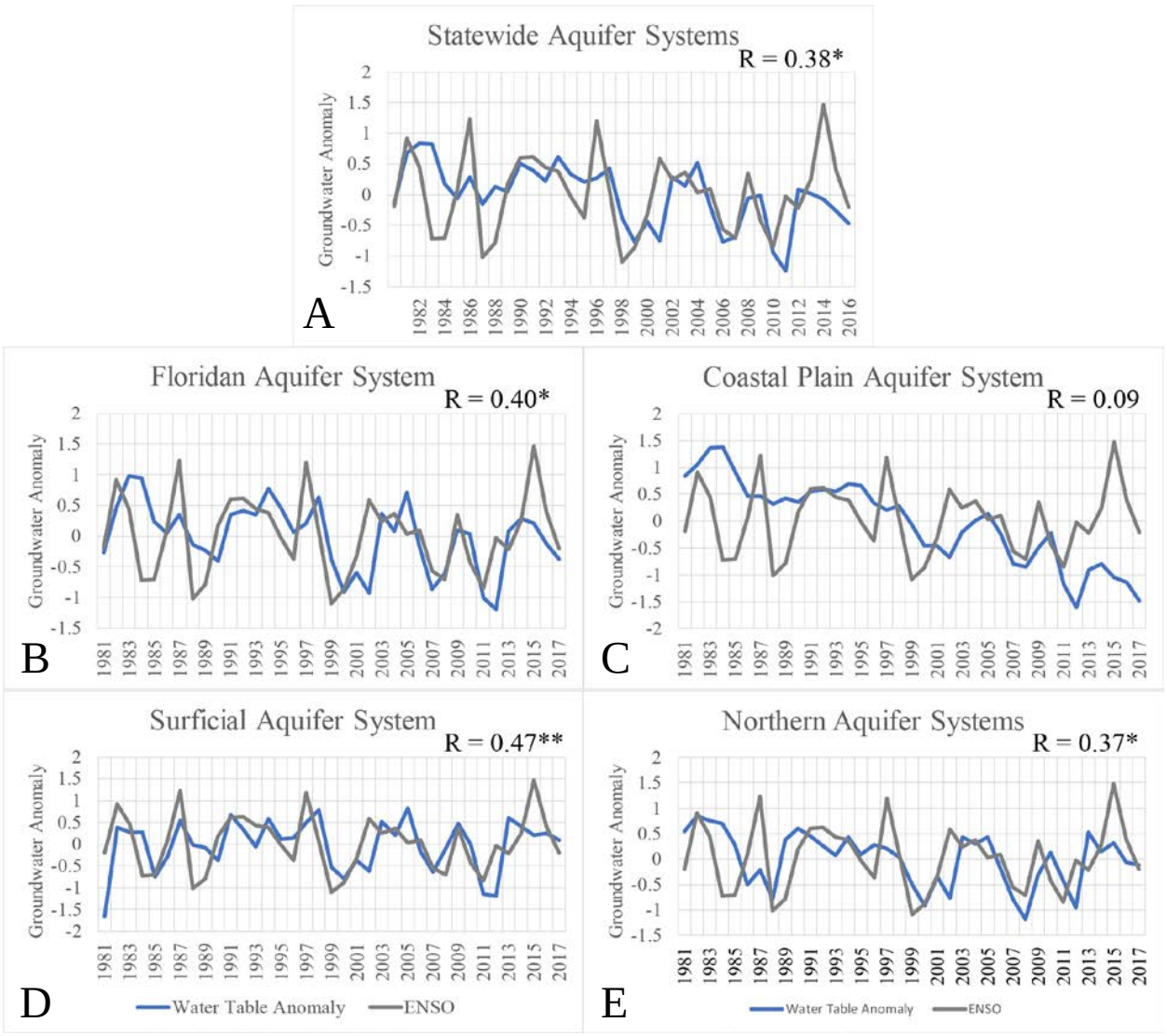

Figure 11. Graph shows annual Georgia groundwater table anomaly (blue) and ENSO anomaly (grey). The two trends show similar increasing and decreasing trends with a slight time lag between ENSO and groundwater fluctuations. Correlation (R) for each set of time series is added to the top right of the chart. P-scores are shown as asterisks (*) beside the R value (*: 95% confidence, **: 99% confidence, ***: 99.9% confidence). A) Shows the statewide time series of average for all four aquifers. (B) Shows the Floridan aquifer system. (C) Shows the Coastal Plain aquifer system. (D) Shows the surficial aquifer system. (E) Shows the Northern aquifer systems.

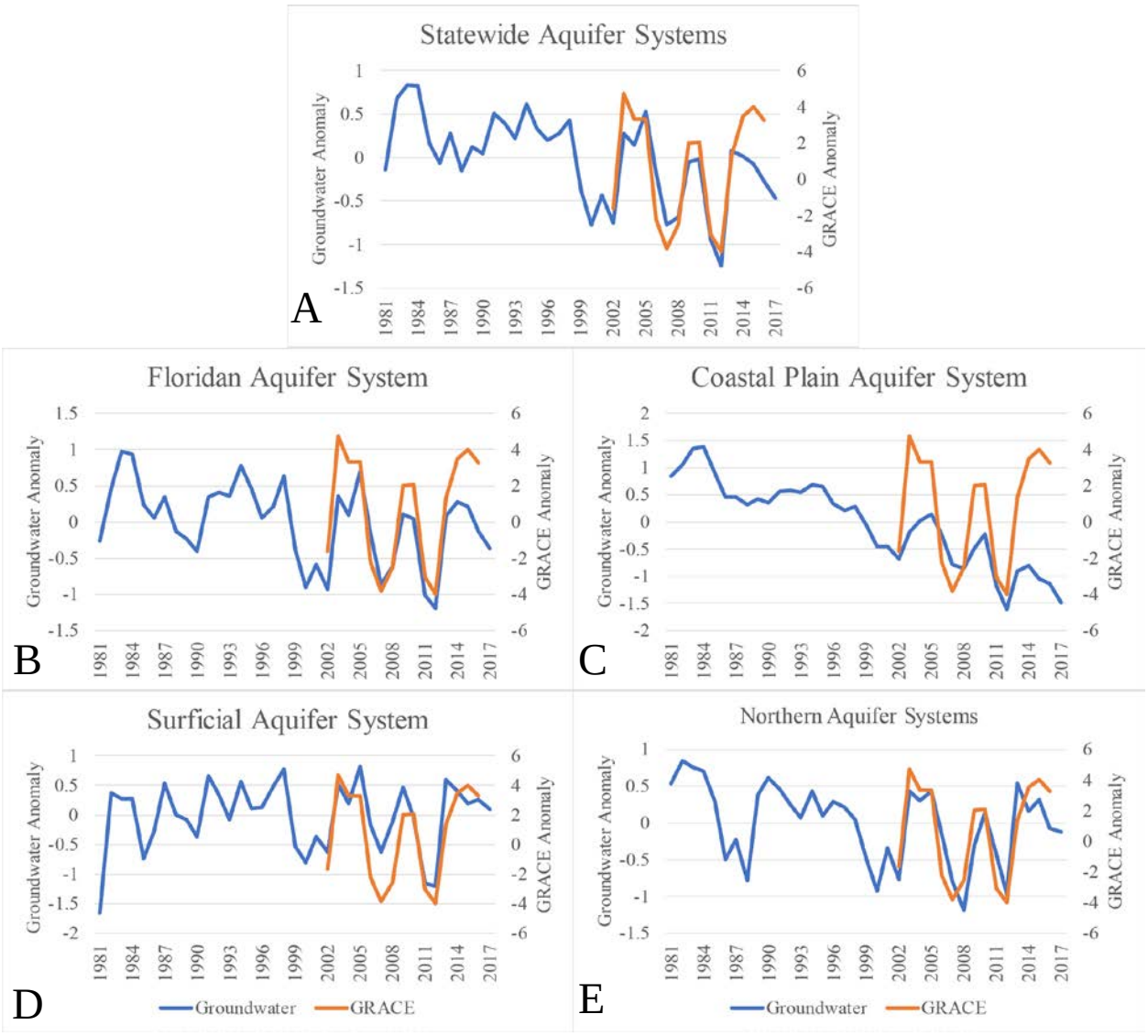

Figure 12. Graph showing groundwater anomaly data for each aquifer and the statewide average (left axis) compared to GRACE data (right axis). GRACE data (orange line) only is available from 2002 to present. Based on the available data, it appears as though GRACE data and groundwater data show similar trends in the observable period. This indicates that groundwater is fluctuating consistently with the GRACE water balance model. A) Shows the statewide average for all four aquifers. (B) Shows the Floridan aquifer system. (C) Shows the Coastal Plain aquifer system. (D) Shows the surficial aquifer system. The surficial aquifer shows the least amount of change over the monitoring period. (E) Shows the Northern aquifer systems.

Autocorrelation Analysis

Figure 12 shows the annual cycle of the autocorrelation function for Georgia groundwater table and annual precipitation anomalies for 1981-2017. Autocorrelation function was calculated for statewide groundwater table average, average for individual aquifer, and statewide precipitation average. Precipitation autocorrelation shows a "memory" of around 3 months, the shortest of any of our analysis. The unconfined SA shows the least amount of memory among various aquifer system, around 6 months for all seasons with a slight increase in memory from May through August. The NAS looks relatively like the SA, but with slightly longer memory from April through December. The FAS shows substantially longer memory than the previous two aquifers with a memory of 12 to 18 months depending on season. Lastly, the confined CPAS shows the longest memory with a memory of over 24 months across all months. The values for each month and aquifer are located in table 6.

The NAS and FAS show trends where the autocorrelation approaches zero and then "reemerges" back to statistical significance. Previously, this has been shown to indicate that deeper soil layers with more memory have forced a longer memory in the shallower layers (Kumar et al. 2019). Similarly, seasonally-varying processes have been shown to provide long-term thermal anomalies in extratropical oceans (Alexander and Desser 1995, Alexander et al. 1999, Deser et al. 2003). Potential reemergence of groundwater occurs in both the FAS and NAS between 12 and 18 months.

Reemergence is the strongest from late summer through winter months (JAS through DJF). The FAS has strong correlation from the JAS season with an 17-month lead through the NDJ season with a 14-month lead. This indicates that the correlation of the JAS season groundwater table anomaly with the groundwater table anomaly of the DJF groundwater table anomaly 17-

months later (e.g., JAS 2015 anomaly correlating with DJF 2016-2017 anomaly). A similar correlation is seen in the NAS where a strong correlation can be seen from the MJJ season through the NDJ season. Both aquifers also show negative reemergence which is likely the same signal but from the past.

Table 6. Table showing the amount of months at which each aquifer loses statistical significance for the autocorrelation analysis. For example, the FAS loses statistical significance 9.56 months after January. Therefore, statistical significance is lost during October for this example.

Month	FAS	CPAS	SA	NAS
January	9.56	24	3.72	10.74
February	9.63	24	4.38	9.08
March	10.46	24	4.41	8.32
April	11.15	24	4.41	7.75
May	11.31	24	4.61	8.51
June	11.52	24	4.66	9.10
July	11.71	24	4.96	8.48
August	11.73	24	5.05	9.01
September	11.50	24	4.84	10.60
October	11.11	24	4.43	11.11
November	10.60	24	4.11	10.76
December	10.14	24	4.15	10.95

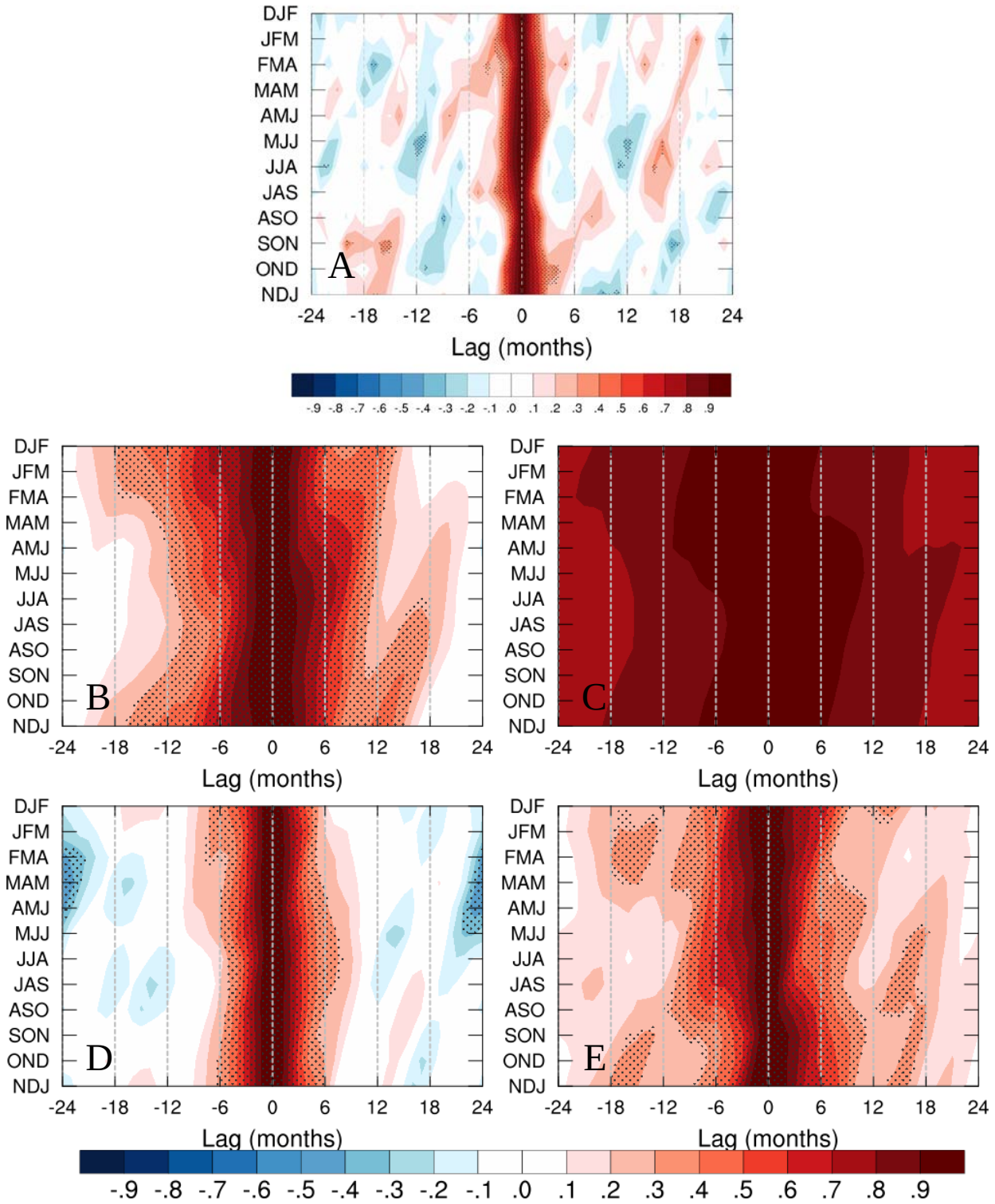

Figure 14. Autocorrelation function of Georgia groundwater table for four aquifers and precipitation. Anomalies are departures from the monthly seasonal cycle, smoothed with a 3-month running mean. Autocorrelation lag is measured from a base 3-month anomaly. For example, a lead of 6 months at NDJ represents correlation between NDJ and the subsequent MJJ season. Plots show the annual cycle of the autocorrelation function for 3-month running mean (A) precipitation, (B) Floridan aquifer system, (C) Coastal Plain aquifer system, (D) Surficial aquifer system, and (E) Northern aquifer systems. The vertical axis shows the time of the base season and the horizontal axis shows the lead/lag.

Figure 15. Autocorrelation function of Georgia groundwater table for four aquifers and precipitation. Anomalies are

Chapter 5: Discussion

Time series water tab;e analysis and GRACE data have shown that groundwater storage appears to be decreasing across Georgia from 1981 to present. There appears to be two different processes affecting how various groundwater aquifer systems are connected to climate in Georgia. The climatically-coupled SA and NAS appear to be largely unaffected by the non-climatic process (e.g., irrigation) that is causing the water table decline. Both aquifers show no significant P scores in the trend analysis (Table 3) and are both correlated to precipitation and ENSO (Table 5). Furthermore, the FAS is shown to be correlated with precipitation and ENSO, but also shows significant Z scores in the trend analysis (Table 3), indicating that annual average and minimum declines most likely cannot be attributed to climate. On the contrary, the CPAS has the least significant precipitation and ENSO correlation (Table 5) and the most significant declining trend. This would indicate that climate has the least effect on the water table of deep aquifers that show the most significant decreasing trend.

Increases in the ENSO index during El Nino episodes typically lead to statewide increases in the groundwater table; decreases in ENSO index during La Nina phase typically lead to decreases in groundwater table with the only exception being from 2013 to 2017. This pattern of groundwater table increase while ENSO index is positive and groundwater decrease while ENSO index is negative has been shown in other studies of the Upper Floridan aquifer in Southwest Georgia (Singh et al., 2015). This analysis appears to show the relationship is valid statewide not only in the Upper Floridan aquifer, but also in the surficial aquifer and the northern aquifer systems.

The autocorrelation analysis shows similar results to the time series analysis and the Mann-Kendall analysis. The unconfined SA especially and the largely unconfined NAS to a less extent

share similar memory with precipitation. By contrast the deeper FAS and the CPAS have significantly longer memory than two other aquifer systems and the climatic drivers of recharge. The longer memory may reflect the longer residence time and mixing processes in the deeper aquifers. Significantly longer memory in deeper, more confined aquifers leads to a decoupling of the aquifer from the climate forcing in this case.

Previous study from Kumar et al (2019) indicated that deeper soil layers with a longer memory may influence the memory in the shallower layers.. My study, however, lacks the data to be able to quantify a reemergence mechanism in groundwater. Potential memory reemergence of groundwater occurs in the FAS aquifer between 12 and 18 months. A possible explanation for the reemergence in the FAS could be due to the residence time of recharge from seasons of higher precipitation. The NAS are not underlain by the CPAS and varies hydrogeologically from the other three aquifers.

Spatial distribution of monitoring well locations show most of the wells analyzed are clustered in the southern and southwestern portions of Georgia. This corresponds to the highly irrigated region (Fig. 2B). Irrigation and evapotranspiration have been shown to significantly reduce overall water storage in Georgia (Mitra et al., 2019). Except for the coastal region, all the wells show decreasing trends in annual average, maximum, and minimum when LTP is considered and only one well does not show decreasing trends when STP is considered. The only statistics that show an overall increasing trend is annual range of water table. Range measures the variation between maximum and minimum. The maximum and minimum are both decreasing, but the minimum is decreasing faster; therefore, the range between the water table high and low is increasing over time. This leads to a statewide increase in the range of the water table, indicating unreliable water availability (Kumar et al., 2014).

Chapter 6: Conclusions

Groundwater table elevation data from 43 groundwater USGS monitoring wells having long term data (37 years) were analyzed for their long-trend and their possible climatic and non-climatic (irrigation) drivers . Statistical analysis used in this study include time series analysis, two variations of Mann-Kendall trend test to consider both short- and long-term serial correlation, and the annual cycle of the autocorrelation function. This study attempted to systematically determine the relationship between climate variability, groundwater table fluctuation, and anthropogenic forcings in Georgia.

Results of time series analysis indicated that groundwater levels have been decreasing on average across Georgia. Further investigation into individual aquifers reveal that each aquifer has responded differently to groundwater depletion influences. The SA and NAS show neutral reactions across the state consistent with the precipitation variations, while the FAS and CPAS show moderate to severe groundwater depletion. Relationships between different aquifers and climatic variables correspond with previous work in Georgia (Mitra et al. 2014). The shallower SA and NAS correspond to changes in precipitation and ENSO. The deeper, but hydrologically interconnected FAS shows some coupling with climate factors and other influences. The deepest confined CPAS appears to be completely decoupled from climate influences and shows the strongest declines.

Mann-Kendall trend analysis shows spatial distribution of statistically significant water table declining trend to be in the southern and southwestern portion of Georgia with the most active irrigation. Mann-Kendall trend analysis of precipitation and streamflow show no significant trend especially when LTP is considered. Significant decreases in annual minimum and 7-day minimum water table occur statewide. Annual minimum and 7-day minimum baseflows in rivers have been

shown previously in southwestern Georgia to correspond with an increase in irrigation (Singh et al. 2016). Irrigation induced baseflow minimums could therefore point to irrigation as the cause for the observed groundwater table minimum. The FAS and CPAS show the most significant decreases across most statistics tested. Previous studies have shown the FAS is affected by irrigation withdrawal increases, leading us to conclude that the deeper, even less climatically coupled CPAS is also affected by irrigation (Mitra et al. 2019, Singh et al. 2016, Mitra et al. 2016, Singh et al. 2017, Mitra et al. 2014). A significant number of wells show annual range (of water table fluctuation) increases across Georgia. This is significant because an increase in range indicates that groundwater is becoming increasingly less reliable (Kumar et al., 2014) which has significant implications on future freshwater management.

Annual autocorrelation analysis indicate that each aquifer and precipitation have different durations of memory. The precipitation shows the least memory (< 3 months), less than half that of the SA. This investigation leads us to further conclude that the deeper aquifers are most likely to be affected by a hydrologic factor other than climate. Studies on soil moisture and oceanic thermal anomalies have previously shown climatic decoupling is possible when the system memory is longer than that of the climate variables (Kumar et al. 2019; Alexander and Deser 1995; Alexander et al. 1999; Namias and Born 1970).

Studies have shown that ENSO linked climate variability has remained largely unchanged in the area and water storage decreases are likely caused by increased water withdrawal (Rose, 2009, Seager et al. 2009, Rugel et al. 2011, Singh et al. 2016). Irrigation acreage in the Coastal Plains regions of Georgia have increased by roughly 2000% since 1973 (Williams et al. 2017). Irrigation has caused the FAS to lose storage, change recharge and discharge patterns from aquifers, and cause some streams to change from gaining to losing (Mitra et al. 2018; Singh et al.

2016; Mitra et al. 2016; Singh et al. 2017; Mitra et al. 2014). The results indicate that the groundwater withdrawals from the FAS and CPAS has resulted in decreased groundwater storage over time statewide.

Overall, this study provides an elaborate view of past groundwater table trends in various Georgia aquifer systems that are in agreement with previous regional work in southwest Georgia. By combining time series analysis, STP and LTP correlation trends, and annual phase autocorrelation, future researches will have a better understanding of the number and significance of wells showing statistically meaningful trends in Georgia. Likewise, by incorporating streamflow and precipitation trends, this study provides a clearer understanding of how climatic and anthropogenic forcings affect different aquifers at different depths and hydrogeologic conditions. A key limitation of this study is the lack of available data in some areas such as the northern part of the state. This study provides a base for additional research to address groundwater trends throughout the southeastern U.S. and other regions. Addressing the factors that influence groundwater fluctuations is critical to understanding how freshwater supply could change in response to natural and anthropogenic forcings in the future.

Literature Cited

Alexander, M., Deser, C., 1995. A Mechanism for the Recurrence of Wintertime Midlatitude SST Anomalies. J. Phys. Oceanogr., 25, 122-137.

Alexander, M., Deser, C., Timlin, M.S., 1999. The Reemergence of SST Anomalies in the North Pacific Ocean. American Meteorological Society 12, 2419-2433.

Alley, W.M., Reilly, T.E., Franke, O.L., 1999, Sustainability of ground-water resources: U.S. Geological Survey Circular 1186, 79 p.

Amenu, G., Kumar, G.P., Liang, X.Z., 2005. Interannual variability of deep-layer hydrologic memory and mechanisms of its influence on surface energy fluxes. J Climate, 18, 5024-5045.

Aziz, O.I.A., Burn, D.H., 2006. Trends and variability in the hydrological regime of the Mackenzie River Basin. Journal of Hydrology 319 (1–4), 282–294.

Braneon, C., 2014. Agricultural Water Demand Assessment in the Southeast U.S. Under Climate Change (Doctoral dissertation). Georgia Institute of Technology, 240 p.

Bates, B., Kundzewicz, Z.W., Wu, S., Palutikof, J.P., 2008. Climate Change and Water. Technical Paper VI of the Intergovernmental Panel on Climate Change. Intergovernmental Panel on Climate Change Secretariat, Geneva, 210 p.

Birsan, M.V., Molnar, P., Burlando, P., Pfaundler, M., 2005. Streamflow trends in Switzerland. Journal of Hydrology 314 (1–4), 312–329.

Brekke, L.D., Kiang, J.E., Olsen, J.R., Pulwarty, R.S., Raff, D.A., Turnipseed, D.P., Webb, R.S., White, K.D., 2009, Climate change and water resources management—A federal perspective: U.S. Geological Survey Circular 1331, 65 p.

Burnett, W.C., Aggarwal, P.K., Aureli, A., Bokuniewicz, H., Cable, J.E., Charette, M.A., Kontar, E., Krupa, S., Kulkarni, K.M., Loveless, A., Moore, W.S., Oberdorfer, J.A., Oliveira, J., Ozyurt, N., Povinec, P., Privitera, A.M.G., Rajar, R., Ramessur, R.T., Scholten, J., Stieglitz, T., Taniguchi, M., Turner, J.V., 2006. Quantifying submarine groundwater discharge in the coastal zone via multiple methods. Sci. Total Environ. 367 (2–3), 498–543.

Chandler, R.V., Gillett, B., DeJarnette, S., 1996, Hydrogeologic and water-use data for southern Baldwin County, Alabama, Geological Survey of Alabama Circular 199, 124.

Chandler, R.V., Moore, J.D., Gillett, B., 1985, Groundwater chemistry and saltwater encroachment, southern Baldwin County, Alabama, Geol. Survey of Alabama Bulletin 126, 166.

Chen, Z., Grasby, S.E., Osadetz, K.G., 2002. Predicting average annual groundwater levels from climatic variables: an empirical model. J. Hydrol. 260 (1–4), 102–117.

Chen, Z., Grasby, S.E., Osadetz, K.G., 2004. Relation between climate variability and groundwater levels in the upper carbonate aquifer, southern Manitoba, Canada. J. Hydrol. 290 (1–2), 43–62.

Chiew, F.H.S., McMahon, T.A., 2002. Modelling the impacts of climate change on Australian streamflow. Hydrol. Process. 16 (6), 1235–1245.

Chikamoto, Y., Timmermann, A.,Stevenson, S., DiNezio, P., Langford, S., 2015. Decadal predictability of soil water, vegetation, and wildfire frequency over North America. Clim Dynam, 45, 2213-2235.

Clarke, J.S., Pierce, R.R., 1985, Georgia groundwater resources, in U.S. Geological Survey, National Water Summary, 1984: U.S. Geological Survey Water-Supply Paper 2275, p. 179–184.

Cohn, T.A., Lins, H.F., 2005. Nature's style: naturally trendy. Geophysical Research Letters 32, L23402. doi:10.1029/2005GL024476.

Cook, B., Shukla, S., Puma, M., Nazarenko, L., 2014. Irrigation as an historical climate forcing, Climate Dynamics, 44:1715–1730.

Daly, C., Taylor, G., Gibson, W., 1997. The prism approach to mapping precipitation and temperature, paper presented at 10th Conference on Applied Climatology, American Meteorological Society, Reno, Nev.

Daly, C., Taylor, G. H., Gibson, W. P., Parzybok, T., Johnson, G. L., Pasteris, P. A., 1998. Development of high quality spatial datasets for the United States, paper presented at First International Conference on Geospatial Information in Agriculture and Forestry, ERIM, Lake Buena Vista, Fla.

Delworth, T. L., Manabe, S., 1988. The Influence of Potential Evaporation on the Variabilities of Simulated Soil Wetness and Climate. J Climate, 1.

Denizman, C., 2018. Land use changes and groundwater quality in Florida. Applied Water Science. 8: 134. https://doi.org/10.1007/s13201-018-0776-9

Deser, C., Alexander, M.A., Timlin, M.S., 2003. Understanding the persistence of sea surface temperature anomalies in midlatitudes. J Climate, 16, 57-72.

Diem JE., 2006. Synoptic-scale controls of summer precipitation in the Southeastern United States. J. Climate 19: 613 – 621, DOI:10.1175/JCLI3645.1.

Diem JE., 2013. Influences of the Bermuda High and atmospheric moistening on changes in summer rainfall in the Atlanta, Georgia region, USA. Int. J. Climatol. 33: 160 – 172, DOI: 10.1002/joc.3421.

Dixon, H., Lawler, D.M., Shamseldin, A.Y., 2006. Streamflow trends in western Britain. Geophysical Research Letters 33, L19406. doi:10.1029/2006GL027325.

Doll, P., 2002. Impact of Climate Change and Variability on Irrigation Requirements: A Global Perspective. Climate Change 54:269-293.

Dragoni, W., Sukhija, B.S., 2008. Climate change and groundwater—A short review, in Dragoni, W., and Sikhija, B.S., eds., Climate change and groundwater: London, Geological Society, Special Publications v. 288, p. 1–12.

Fan, Y., Duffy, C.J., Oliver, J.D.S., 1997. Density-driven groundwater flow in closed desert basins: field investigations and numerical experiments. J. Hydrol. 196 (1–4), 139–184.

Fanning, J.L., 2003. Water use in Georgia by county for 2000 and water-use trends for 1980–2000: Georgia Geologic Survey Information Circular 106, 176 p.

Ford, T., Labosier C.F., 2014. Spatial patterns of drought persistence in the Southeastern United States. International Journal of Climatology 34: 2229-2240.

GADNR, 2006. Coastal Georgia Water & Wastewater Permitting Plan for Managing Salt Water Intrusion. https://www1.gadnr.org/cws/Documents/saltwater_management_plan_june2006.pdf

Georgakakos, A. P., Zhang, F., Yao, H., 2010. Climate Variability and Change Assessment for the ACF River Basin, Southeast US. Georgia Water Resources Institute (GWRI) Technical Report sponsored by NOAA, USGS, and Georgia EPD, 321 pp., Georgia Institute of Technology, Atlanta, GA.

Ghannam, K., Nakai, T., Paschalis, A., Oishi, C., Kotani, A., Igarashi, Y., Kumagai, T., Katul, G.G., 2016. Persistence and memory timescales in root-zone soil moisture dynamics. Water Resour Res, 52, 1427-1445.

Gillett, B., Raymond, D.E., Moore, J.D., Tew, B.H., 2000. Hydrogeology and vulnerability to contamination of major aquifers in Alabama: area 13. Geological Survey of Alabama circular 199A

Gordon, D.W., Painter, J.A., 2018. Groundwater conditions in Georgia, 2015–16: U.S. Geological Survey Scientific Investigations Report 2017–5142, 59 p., https://doi.org/10.3133/sir20175142.

Green, T.R., Taniguchi, M., Kooi, H., 2007. Potential impacts of climate change and human activity on subsurface water resources: Vadose Zone Journal, v. 6, no. 3, p. 531–532.

Green, T. R., Taniguchi, M., Kooi, H., Gurdak, J.J., Allen, D.M., Hiscock, K.M., Treidel, H., Aureli, A., 2011. Beneath the surface of global change: Impacts of climate change on groundwater. J. Hydrol. 405, 532–560.

Guo, D., 2008. Regionalization with dynamically constrained ag-glomerative clustering and partitioning (REDCAP). International 642 Journal of Geographical Information Science 22(7), 801–823.

Gurdak, J.J., Hanson, R.T., McMahon, P.B., Bruce, B.W., McCray, J.E., Thyne, G.D., R.C. Reedy, 2007. Climate variability controls on unsaturated water and chemical movement, High Plains aquifer, USA: Vadose Zone Journal, v. 6, no. 3, p. 533–547.

Gurdak, J.J., Hanson, R.T., Green, T.R., 2009. Effects of climate variability on groundwater resources of the United States: U.S. Geological Survey Fact Sheet 2009-3074, 4 p.

Hamed, K.H., 2008. Trend detection in hydrologic data: the Mann–Kendall trend test under the scaling hypothesis. Journal of Hydrology 349, 350–363.

Hamed, K.H., Rao, A.R., 1998. A modified Mann–Kendall trend test for autocorrelated data. Journal of Hydrology 204, 182–196.

Hanson, R.T., Dettinger, M.D., 2005. Ground water/surface water responses to global climate simulations, Santa Clara-Calleguas basin, Ventura, California. J. Am. Water Resour. Assoc. 41 (3), 517–536.

Hanson, R.T., Dettinger, M.D., Newhouse, M.W., 2006. Relations between climatic variability and hydrologic time series from four alluvial basins across the southwestern United States. Hydrogeol. J. 14 (7), 1122–1146.

Hanson, R.T., Martin, P., Koczot, K.M., 2003. Simulation of ground water/surface water flow in the Santa Clara–Calleguas Basin, Ventura County, California: U.S. Geological Survey Water-Resources Investigations Report 2002–4136, 214 p.

Hanson, R.T., Newhouse, M.W., Dettinger, M.D., 2004. A methodology to assess relations between climatic variability and variations in hydrologic time series in the southwestern United States. J. Hydrol. 287 (1–4), 252–269.

Hatcher, R. D. Jr., 1978. Tectonics of the western Piedmont and Blue Ridge, southern Appalachians : review and speculation. Am. J. Sci. 278 : 276-304

Holman, I.P., 2006. Climate change impacts on groundwater recharge-uncertainty, shortcomings, and the way forward? Hydrogeol. J. 14 (5), 637–647.

Hurst, H.E., 1951. Long term storage capacities of reservoirs. Transactions of the American Society of Civil Engineers 116, 776–808.

Joelson, M., Golder, J., Beltrame, P., Néel, M.-C., Di Pietro, L., 2016. On fractal nature of groundwater level fluctuations due to rainfall process, Chaos Soliton. Fract., 82, 103–115.

Ingram, K., Dow, K., Carter, L., Anderson, J., 2013. Climate of the Southeast United States: Variability, change, impacts, and vulnerability. Washing DC: Island Press.

IPCC, 2014: Climate Change 2014: Impacts, Adaptation, and Vulnerability. Part B: Regional Aspects. Contribution of Working Group II to the Fifth Assessment Report of the Intergovernmental Panel on Climate Change [Barros, V.R., C.B. Field, D.J. Dokken, M.D. Mastrandrea, K.J. Mach, T.E. Bilir, M. Chatterjee, K.L. Ebi, Y.O. Estrada, R.C. Genova, B. Girma, E.S. Kissel, A.N. Levy, S. MacCracken, P.R. Mastrandrea, and L.L. White (eds.)]. Cambridge University Press, Cambridge, United Kingdom and New York, NY, USA, 688 pp. Karl, T.R., Jerry, M.M., Peterson, T.C., Susan, J.H., 2009. Global Climate Change Impacts in the United States; Cambridge University Press: Cambridge, UK.

Kendall, M.G., 1975. Rank Correlation Methods. Griffin, London

Koutsoyiannis, D., 2003. Climate change, the Hurst phenomenon, and hydrological statistics. Hydrological Sciences-Journal-des Sciences Hydrologiques 48 (1).

Koutsoyiannis, D., Montanari, A., 2007. Statistical analysis of hydroclimatic time series: uncertainty and insights. Water Resources Research 43, W05429. doi:10.1029/2006WR005592

Kruger, A., Ulbrich, U., Speth, P., 2001. Groundwater recharge in Northrhine-Westfalia predicted by a statistical model for greenhouse gas scenarios. Phys. Chem. Earth 26 (11–12), 853–861.

Kumar S., Merwade, V., Kam, J., Thurner, K., 2009. Streamflow trends in Indiana: effects of long term persistence, precipitation and subsurface drains. Journal of Hydrology, 374, 171–183.

Kumar S., Merwade, V., Lee, W., Zhao, L., Song, C., 2010. Hydroclimatological impact of century-long drainage in midwestern United States: CCSM sensitivity experiments. J. Geophys. Res. 115, D14105, doi:10.1029/2009JD013228.

Kumar S., Merwade, V., Niyogi, D., Kinter III, J. L., 2013. Evaluation of temperature and precipitation trends and long-term persistence in CMIP5 20th century climate simulations. J. Clim., doi:10.1175/JCLI-D-12-00259.1

Kumar S., Lawrence, D. M., Dirmeyer, P. A., Sheffield, J., 2014. Less reliable water availability in the 21st century climate projections, Earth's Future, 2, 152–160, doi:10.1002/2013ef000159.

Kumar S., Newman, M., Wang, Y., Livneh, B., 2019. Potential reemergence of seasonal soil moisture anomalies in North America. J. Climate. doi:10.1175/JCLID-18-0540.1, in press.

Kundzewicz, Z.W., Mata, L.J., Arnell, N.W., Doll, P., Kabat, P., Jimenez, B., Miller, K.A., Oki, T., Sen, Z., Shiklomanov, I.A., 2007. Freshwater resources and their management. In: Parry, M.L., Canziani, O.F., Palutikof, J.P., van der Linden, P.J., Hanson, C.E. (Eds.), Climate Change 2007: Impacts, Adaptation and Vulnerability. Cambridge University Press, Cambridge, p. 173–210.

Kunkel, K. E., Stevens, L. E., Stevens, S. E., Sun, L., Janssen, E., Wuebbles, D., Konrad II, C. E., Fuhrman, C. M., Keim, B. D., Kruk, M. C., Billet, A., Needham, H., Schafer, M., Dobson, J. G., 2013. Regional Climate Trends and Scenarios for the U.S. National Climate Assessment: Part 2. Climate of the Southeast U.S. NOAA Technical Report 142-2. 103 pp., National Oceanic and Atmospheric Administration, National Environmental Satellite, Data, and Information Service, Washington D.C.

Labosier C.F, Quiring S.M., 2013. Hydroclimatology of the Southeastern USA. Climate Res. 57: 157 – 171, DOI: 10.3354/cr01166.

Landerer F.W., Swenson S. C., 2012. Accuracy of scaled GRACE terrestrial water storage estimates. Water Resources Research, Vol 48, W04531, 11 PP, doi:10.1029/2011WR011453.

Lee, K.S., Chung, E.S., 2007. Hydrological effects of climate change, groundwater withdrawal, and land use in a small korean watershed. Hydrologic Processes 21 (22), 3046–3056.

Leeth, D.C., Peck, M.F., and Painter, J.A., 2007. Ground-Water Conditions and Studies in Georgia, 2004– 2005: U.S. Geological Survey Scientific Investigations Report 2007-5017, 299 p., publication available at http://pubs.usgs.gov/sir/2007/5017/.

Lettenmaier, D.P., Wood, E.F., Wallis, J.R., 1994. Hydro-climatological trends in the continental United States, 1948–88. Journal of Climate 7 (4), 586–607.

Lins, H.F., Slack, J.R., 1999. Streamflow trends in the United States. Geophysical Research Letters 26 (2), 227–230.

Loáiciga, H.A., Valdes, J.B., Vogel, R., Garvey, J., Schwartz, H., 1996. Global warming and the hydrologic cycle: Journal of Hydrology, v. 174, no. 1–2, p. 83–127.

Mahmood, R., Pielke, R.A., Hubbard, K.G., Niyogi, D., Dirmeyer, P.A., McAlpine, C., Carleton, A.M., Hale, R., Gameda, S., Beltrán-Przekurat, A., Baker, B., McNider, R., Legates, D.R., Shepherd, M., Du, J., Blanken, P.D., Frauenfeld, O.W., Nair, U.S., Fall, S., 2013. Land cover changes and their biogeophysical effects on climate. Int J Climatol. doi: 10.1002/joc.3736

Mann, H.B., 1945. Non-parametric tests against trend. Econometrica 13, 245–259

McCabe, G.J., Palecki, M.A., Betancourt, J.L., 2004. Pacific and Atlantic ocean influences on multidecadal drought frequency in the United States. Proc. Natl. Acad. Sci. USA 101 (12), 4136–4141.

Melillo, J., Terese, M., Richmond, T.C., and Yohe, G.W., 2014. Climate Change Impacts in the United States: The Third National Climate Assessment. U.S. Global Change Research Program, 841 pp. doi:10.7930/J0Z31WJ2.

Miller, J.A., 1986. Hydrogeologic framework of the Floridan Aquifer System in Florida and in parts of Georgia, Alabama, and South Carolina: U.S. Geological Survey Professional Paper 1403-B, 91 p.

Miller, J. A., 1988. Hydrogeologic framework of the Floridan Aquifer System in Florida and in parts of Georgia, South Carolina, and Alabama: U.S. Geological Survey Professional Paper 1403-B, 91 p.: http://sofia.usgs.gov/publications/papers/pp1403b/pdf%5Findex.html (July 2008).

Renken, R.A., 1996, Hydrogeology of the Southeastern Coastal Plain aquifer system in

Mississippi, Alabama, Georgia, and South Carolina: U.S. Geological Survey Professional Paper 1410–B, 101 p., 142 pls.

Miller, N.L., Dale, L.L., Brush, C.F., Vicuna, S.D., Kadir, T.N., Dogrul, E.C., Chung, F.I., 2009. Drought resilience of the California Central Valley surface-ground-water-conveyance system. J. Am. Water Resour. Assoc. 45 (4), 857–866.

Milly, P.C.D., Betancourt, J.L., Falkenmark, M., Hirsch, R.M., Kundzewicz, Z.W., Lettenmaier, D.P., Stouffer, R.J., 2008. Stationarity is dead: whither water management? Science 319, 573–574.

Milly, P.C.D., Dunne, K.A., Vecchia, A.V., 2005. Global pattern of trends in streamflow and water availability in a changing climate. Nature 438, 347–350.

Mitra, S., Srivastava, P., Singh, S., Yates, D., 2014. "Effect of ENSO induced climate variability on groundwater levels in the lower Apalachicola–Chattahoochee–Flint River Basin."Trans.ASABE 57(5): 1393–1403. https://doi.org/10.13031/trans.57.10748.

Mitra, S., Srivastava, P., Singh, S., 2016. "Effects of irrigation pumpage on groundwater levels during droughts in the lower Apalachicola– Chattahoochee–Flint River Basin." Journal of Hydrogeology. 24: 1565–1582. https://doi.org/10.1007/s10040-016-1414-y.

Mitra, S., Singh, S., Srivastava, P., 2019. Sensitivity of Groundwater Components to Irrigation Withdrawals during Droughts on Agricultural-Intensive Karst Aquifer in the Apalachicola–Chattahoochee–Flint River Basin. Journal of Hydrologic Engineering. 24. 10.1061/(ASCE)HE.1943-5584.0001688

Murgulet, D., Tick, G., 2008. The extent of saltwater intrusion in southern Baldwin County, Alabama, Environmental Geology, v. 55, number 6, p. 1235-1245.

Namias, J., Born, R.M., 1970. Temporal Coherence in North Pacific Sea-Surface Temperature Patterns. Journal of Geophysical Research, 75, 5952

National Wildlife Federation, 2008. More Variable and Uncertain Water Supply: Global Warming's Wake-Up Call for the Southeastern United States. Water Conservation. 1-8.

NCAR, 2012: The NCAR Command Language (version 6.0.0). UCAR/NCAR/CISL/VETS. [Available online at http://www. ncl.ucar.edu/.]

Novotny, E.V., Stefan, H.G., 2007. Stream flow in Minnesota: indicator of climate change. Journal of Hydrology 334 (3–4), 319–333.

Onoz, B., Bayazit, M., 2003. The power of statistical tests for trend detection. Turkish Journal of Engineering and Environmental Sciences 27 (4), 247–251.

Ouysse, S., Laftouhi, N.E., Tajeddine, K., 2010. Impacts of climate variability on the water resources in the Draa basin (Morocco): analysis of the rainfall regime and groundwater recharge. In: Taniguchi, M., Holman, I.P. (Eds.), Groundwater Response to Changing Climate, International Association of Hydrogeologists Selected Paper. CRC Press, Taylor and Francis Group, London, UK, p. 27–48.

Rakhshandehroo, G. R., Amiri, S. M. 2012. Evaluating fractal behavior in groundwater level fluctuations time series, J. Hydrol., 464, 550–556.

Reed, P.C., 1971. Geologic map of Baldwin County, Alabama, Geological Survey Special Map 94:5.

Reilly, T.E., Dennehy, K.F., Alley, W.M.. Cunningham, W.L., 2008. Ground-water availability in the United States: U.S. Geological Survey Circular 1323, 70 p.

Renken, R. A., 1996. Hydrogeology of the southeastern Coastal Plain aquifer system in Mississippi, Alabama, Georgia, and South Carolina, U.S. Geol. Surv. Prof. Pap., 1410-B, 101 p.

Rose, S., 2009. Rainfall runoff trends in the southeastern USA: 1938–2005. Hydrol. Processes 23, 1105–1118.
Rosenberg, N.J., Epstein, D.J., Wang, D., Vail, L., Srinivasan, R., Arnold, J.G., 1999. Possible impacts of global warming on the hydrology of the Ogallala Aquifer region. Clim. Change 42 (4), 677–692.
Rugel, K., Jackson, C.R., Romeis, J.J., Golladay, S.W., Hicks, D.W., Dowd, J.F., 2011. Effects of irrigation withdrawals on streamflows in a karst environment: lower Flint River Basin, Georgia, USA. Hydrol. Processes 26, 523–534, http://dx.doi.org/10.1002/hyp.8149.
Rutledge, A.T., Mesko, T.O., 1996. Estimated hydrologic characteristics of shallow aquifer systems in the Valley and Ridge, the Blue Ridge, and the Piedmont physiographic provinces based on analysis of stream flow recession and base flow. USGS Professional Paper 1422-B, Reston
Sandstrom, K., 1995. Modeling the effects of rainfall variability on groundwater recharge in semi-arid Tanzania. Nordic Hydrol. 26, 313–330.
Schlosser, C. A., Milly, P.C.D., 2002. A model-based investigation of soil moisture predictability and associated climate predictability. J Hydrometeorol, 3, 483-501.
Seager, R., Tzanova, A., Nakamura, J., 2009. Drought in the southeastern United States: causes, variability over the last millennium, and the potential for future hydro climate change. J. Clim. 22, 5021–5045, http://dx.doi.org/10.1175/2009JCLI2683.1.
Sen, P.K., 1968. Estimates of the regression coefficients based on Kendall's tau. Journal of the American Statistical Association 63, 1379–1389.
Sharma, M. L. 1989. `Impact of climate change on groundwater recharge', in Conference on Climate and Water. Publication of the Academy of Finland. Vol. 1, p. 511-520.
Sherif, M.M., Singh, V.P., 1999. Effect of climate changes on seawater intrusion in coastal aquifers: Hydrologic Processes, v. 13, no. 8, p. 1277–1287.
Siebert, S., Döll, P., Hoogeveen, J., Faures, J.M., Frenken, K., Feick, S., 2005. Development and validation of the global map of irrigation areas. Hydrology and Earth System Sciences 9: 535–547.
Singh, S., Srivastava, P., Abebe, A., Mitra, S., 2015. "Baseflow response to climate variability induced droughts in the Apalachicola– Chattahoochee–Flint River Basin, USA." Journal of Hydrology. 528: 550–561. https://doi.org/10.1016/j.jhydrol.2015.06.068.
Singh, S., Srivastava, P., Mitra, S., Abebe. A., 2016. "Climate variability and irrigation impacts on streamflows in a karst watershed—A systematic evaluation." Journal of Hydrology Regional Studies. 8: 274–286. https://doi.org/10 .1016/j.ejrh.2016.07.001.
Singh, S., Mitra, S., Srivastava, P., Abebe, A., Torak, L., 2017. Evaluation of water-use policies for baseflow recovery during droughts in an intensive karst watershed: Case study of the lower Apalachicola-Chattahoochee-Flint River Basin, southeastern United States. Hydrological Processes, 31, 3628-3644.
Sophocleous, M., 2004. Climate change: why should water professionals care? Ground Water 42 (5), 637.
Sophocleous, M., 2010. Groundwater management practices, challenges, and innovations in the High Plains aquifer, USA — lessons and recommended actions. J. Hydrogeol. 18, 559–575.
Sun, G., McNulty, S.G., Myers, J.A.M., Cohen, E.C., 2008. Impacts of multiple stresses on water demand and supply across the southeastern United States. Journal of the American Water Resource Association 44, 1441–1457.

Swenson, S. C., Wahr, J., 2006. Post-processing removal of correlated errors in GRACE data, Geophys. Res. Lett., 33, L08402, doi:10.1029/2005GL025285.
Swenson, S.C., 2012. GRACE monthly land water mass grids NETCDF RELEASE 5.0. Ver. 5.0. PO.DAAC, CA, USA. Dataset accessed [2019/02/15] at http://dx.doi.org/10.5067/TELND-NC005.
Szabo, M. W., Copeland, C. W., Jr., 1988. Geologic map of Alabama: southwest sheet: Alabama Geological Survey Special Map 220
Taylor, K. E., Stouffer, R.J., Meehl, G.A., 2012. An overview of CMIP5 and the experiment design. Bull. Amer. Meteor. Soc., 93, 485–498.
Thiel, H., 1950. A rank-invariant method of linear and polynomial analysis, part 3. Nederlandse Akademie van Wettenschappen, Proceedings 53, 1397–1412.
Thomsen, R., 1989. `The effect of climate variability and change on groundwater in Europe', in Conference on Climate and Water. Publication of the Academy of Finland. Helsinki, Finland, Vol. 1, p. 486-500.
Tilman, D., 1999. Global environmental impacts of agricultural expansion: The need for sustainable and efficient practices, Pro-ceedings of the National Academy of Sciences, 96(11):5995–6000.
Tilman, D., 2001. Forecasting Agriculturally Driven Global Environmental Change. Science, 292(5515), 281–284.
Tu, T., Ercan, A., and Kavvas, M. L., 2017. Fractal Scaling Analysis of Groundwater Dynamics in Confined Aquifers, Earth Syst. Dynamics, 8, 931-949.
USGS, 2006. Fact Sheet 2006-3077: Georgia's Ground-Water Resources and Monitoring Network, 2006. https://pubs.usgs.gov/fs/2006/3077/pdf/fs2006-3077.pdf (accessed December 3, 2018).
USGS, 2006. National water information system. http://waterdata.usgs.gov/nwis (accessed May 17, 2018).
Van Dijck, S.J.E., Laouina, A., Carvalho, A.V., Loos, S., Schipper, A.M., Van der Kwast, H., Nafaa, R., Antari, M., Rocha, A., Borrego, C., Ritsema, C.J., 2006. Desertification in northern Morocco due to effects of climate change on groundwater recharge. In: Kepner, W.G., Rubio, J.L., Mouat, D.A., Pedrazzini, F. (Eds.), Desertification in the Mediterranean region: A Security Issue. Springer, Dordrecht, The Netherlands, p. 549–577.
von Storch, H., 1995. Misuses of statistical analysis in climate research. In: von Storch, H., Navarra, A. (Eds.), Analysis of Climate Variability: Applications of Statistical Techniques. Springer, Berlin, pp. 11–26.
Warner, S.D., 2007. Climate change, sustainability, and ground water remediation: the connection. Ground Water Monit. Remed. 27 (4), 50–52.
Wang, H., Fu, R., Kumar, A, Li, W.H., 2010. Intensification of summer rainfall variability in the southeastern United States during recent decades. J. Hydrometeorol. 11: 1007 – 1018 doi:10.1175/2010JHM1229.1
Wear, D.N., 2002. Landuse. In: Southern Forest Resources Assessment, D.N. Wear and J.G. Greis (Editors). Gen. Tech. Rep. SRS53 Chapter 6. U.S. Department of Agriculture, Forest Service, Southern Research Station, Asheville, North Carolina, 635 pp.

Williams, L.J., Dixon, J.F., 2015. Digital surfaces and thicknesses of selected hydrogeologic units of the Floridan aquifer system in Florida and parts of Georgia, Alabama, and South Carolina: U.S. Geological Survey Data Series 926, 24 p., http://dx.doi.org/10.3133/ds926.

Williams, M.D., Hawley, C., Madden, M., Shepherd J.M., 2017. Mapping the Spatio-Temporal Evolution of Irrigation in the Coastal Plain of Georgia, USA. Remote Sensing. 83(1):57-67 p.

Wolter, K., Timlin, M.S., 1993. Monitoring ENSO in COADS with a seasonally adjusted principle component index. p. 52–57. In Proc. of the 17th Climate Diagnostic Workshop, Norman, OK. NOAA/N MC/CAC, NSSL, Oklahoma Clim. Survey, CIMMS. and the School of Meteor., Univ. of Oklahoma.

Wolter, K., Timlin, M.S., 1998. Measuring the strength of ENSO: How does 1997/1998 rank? Weather 53:315-324

Yue, S., Pilon, P., Phinney, B., Cavadias, G., 2002. The influence of autocorrelation on the ability to detect trend in hydrological series. Hydrological Processes 16 (9), 1807–1829.

Appendix 1-10: Data Management/NCL Code

The code that was written for this study is presented at the following “Box” URL (https://auburn.box.com/s/qo17ard4rnl98gloxdibufclapszdmrw). Each code is labeled as Appendix 1, 2 ,3, etc. corresponding with the order in which it appears in the text.